AD-768 710

SEISMIC REFRACTION EXPLORATION FOR ENGINEERING SITE INVESTIGATIONS

Bruce B. Redpath

Explosive Excavation Research Laboratory Livermore, California

May 1973

26362-01 rev A
6/5/96

KEEP UP TO DATE

Between the time you ordered this report which is only one of the hundreds of thousands in the NTIS information collection available to you - and the time you are reading this message, several *new* reports relevant to your interests probably have entered the collection.

Subscribe to the **Weekly Government Abstracts** series that will bring you summaries, of new reports as soon as they are *received by NTIS* from the originators of the research. The WGA's are an NTIS weekly newsletter service covering the most recent research findings in 25 areas of industrial, technological, and sociological interest - invaluable in formation for executives and professionals who must keep up to date.

The executive and professional information service provided by NTIS in the **Weekly Government Abstracts** newsletters will give you thorough and comprehensive coverage of government-conducted or sponsored research activities. And you'll get this important information within two weeks of the time it's released by originating agencies.

WGA newsletters are computer produced and electronically photocomposed to slash the time gap between the release of a report and its availability. You can learn about technical innovations immediately - and use them in the most meaningful end productive ways possible for your organization. Please request NTIS-PR-205/PCW for more information.

The weekly newsletter series will keep you current. But learn what you have missed in the past by ordering a computer NTISearch of all the research reports in your area of interest, dating as far back as 1964, if you wish. Please request NTIS-PR-186/PCN for more information.

WRITE: Managing E Editor
5285 Port Royal Road
Springfield, VA 22161

Keep Up To Date With SRIM

SRIM (Selected Research in Microfiche) provides you with regular, automatic distribution of the complete texts of NTIS research reports only in the subject areas you select. SRIM covers almost all Government research reports by subject area and/or the originating Federal or local government agency. You may subscribe by any category or subcategory of our WGA **(Weekly Government Abstr acts)** or **Government Reports Announcements and Index** categories, or to the reports issued by a particular agency such as the Department of Defense, Federal Energy Adminisitration, or Environmental Protection Agency. Other options that will give you greater selectivity are available on request.

The cost of SRIM service is only 45¢ ice, domestic (60¢ foreign) for each complete microfiched report. Your SRIM service begins as soon as your order is received and processed and you will receive biweekly shipments thereafter. If you wish, your service will be backdated to furnish you microfiche of reports issued earlier.

Because of contractual arrangements with several Special Technology Groups, not all NTIS reports are distributed in the SRIM program. You will receive a notice in your microfiche shipments identifying the exceptionally priced reports not available through SRIM.

A deposit account with NTIS is required before this service can be initiated. If you have specific questions concerning this service, please call (703) 451-1558, or write NTIS, attention SRIM Product Manager.

This information product distributed by

NTIS

U.S. DEPARTMENT OF COMMERCE
National Technical Information Service
5285 Port Royal Road
Springfield, Virginia 22161

UNCLASSIFIED

Security Classification

AD 768 710

DOCUMENT CONTROL DATA - R & D

(Security classification of title, body of abstract and indexing annotation must be entered when the overall report is classified)

1. ORIGINATING ACTIVITY (Corporate author)

U. S. Army Engineer Waterways Experiment Station Explosive Excavation Research Laboratory

2a. REPORT SECURITY CLASSIFICATION

UNCLASSIFIED

2b. GROUP

3. REPORT TITLE

Seismic Refraction Exploration for Engineering Site Investigations

4. DESCRIPTIVE NOTES (Type of report and inclusive dates)

Technical Report

5. AUTHOR(S) (First name, middle initial, last name)

Bruce B. Redpath

6. REPORT DATE

May 1973

7a. CONTRACT OR GRANT NO.

b. PROJECT NO.

c.

d.

8a. ORIGINATOR'S REPORT NUMBER(S)

TR E-73-4

8b. OTHER REPORT NO(S) (Any other numbers that may be assigned this report)

10. DISTRIBUTION STATEMENT

Approved for public release; distribution unlimited.

11. SUPPLEMENTARY NOTES

12. SPONSORING MILITARY ACTIVITY

Directorate of Military Construction, OCE DAEN-MCE-D

13. ABSTRACT

This report is a summary of the theory and practice of using the refraction seismograph for shallow, subsurface investigations. It is intended to be a guide to the application of the technique and not a comprehensive analysis of every aspect of the method. The report begins with the fundamentals and then progresses from time-intercept calculations to interpretations using delay times. The limitations of this exploration tool are discussed, and other applications of the equipment, such as uphole surveys, are described. The report also recommends field procedures for carrying out refraction surveys.

DD FORM 1 NOV 68 1473

UNCLASSIFIED

Security Classification

UNCLASSIFIED

Security Classification

14. KEY WORDS	LINK A		LINK B		LINK C	
	ROLE	WT	ROLE	WT	ROLE	WT
Seismic Refraction						
Shallow Exploration						
Site Investigation						

☆ GPO 791-881

UNCLASSIFIED

Security Classification

Destroy this report when no longer needed.
Do not return it to the originator.

The findings in this report are not to be construed as an official Department of the Army position unless so designated by other authorized documents.

Printed in USA. Available from Defense Documentation Center,
Cameron Station, Alexandria, Virginia 22314 or
National Technical Information Service,
U. S. Department of Commerce
Springfield, Virginia 22151

TID-4500, UC-35
Peaceful Applications
of Explosions

TECHNICAL REPORT E-73-4
SEISMIC REFRACTION EXPLORATION FOR ENGINEERING SITE INVESTIGATIONS

BRUCE B. REDPATH

U. S. ARMY ENGINEER WATERWAYS EXPERIMENT STATION
EXPLOSIVE EXCAVATION RESEARCH LABORATORY
Livermore, California

MS. date: May 1973

Foreword

This report was prepared by the U. S. Army Engineer Waterways Experiment Station (USAEWES) Explosive Excavation Research Laboratory (EERL), formerly the Explosive Excavation Research Office (EERO) from 1 August 1971 until 21 April 1972. Prior to 1 August 1971 the organization was known as the USAE Nuclear Cratering Group.

The report was sponsored and funded under RDT&E 21X2040 P562G by the Directorate of Military Construction, Office of the Chief of Engineers (DAEN-MCE-D).

The Director of the Waterways Experiment Station during the preparation of this report was COL Ernest D. Peixotto; the Directors of EERL were LTC Robert L. LaFrenz and LTC Robert R. Mills, Jr.

Abstract

This report is a summary of the theory and practice of using the refraction seismograph for shallow, subsurface investigations. It is intended to be a guide to the application of the technique and not a comprehensive analysis of every aspect of the method. The report begins with the fundamentals and then progresses from time-intercept calculations to interpretations using delay times. The limitations of this exploration tool are discussed, and other applications of the equipment, such as uphole surveys, are described. The report also recommends field procedures for carrying out refraction surveys.

Acknowledgments

Messrs. Bruce Hall and Vincent Gottschalk monitored the project for the Directorate of Military Construction, Office of the Chief of Engineers (DAEN-MCE-D), and the author is grateful for their helpful suggestions and their patience. The author also wishes to thank Messrs. Paul Fisher and Wayne McIntosh of the Geology Branch, Engineering Division, Office of the Chief of Engineers, and Messrs. Sigmund Schwarz and Boyd Bush of Shannon & Wilson, Inc., Seattle, for all of their valuable comments and constructive criticism of the report.

Conversion factors

British units of measurement used in this report can be converted to metric units as follows:

Multiply	By	To obtain
feet	0.3048	meters
pounds	0.4535924	kilograms

Contents

FIGURES

FIGURES (continued)

TABLES

SEISMIC REFRACTION EXPLORATION FOR ENGINEERING SITE INVESTIGATIONS

Introduction

PURPOSE

This report is intended as a guide to the application of seismic refraction techniques to shallow, subsurface exploration of engineering sites. Many civil engineers and geologists have some acquaintance with this basic geophysical tool, but few apply it frequently. The primary purpose of the report is to provide the reader with a working knowledge of the method, with a convenient reference, and further, with a basis to judge the applicability of the method and the results to his particular exploration problem.

BACKGROUND

Refraction seismic surveying was the first major geophysical method to be applied in the search for oil bearing structures. Today, however, oil exploration relies almost exclusively on some variety of the modern reflection seismograph. Recent progress in geophysical exploration for oil has stemmed from refinements to instrumentation and from the computer-assisted processing and enhancement of the data. Refraction surveys are still used occasionally in oil exploration, particularly where they can assist in resolving complicated problems in structural geology.

Although its application in the oil industry has diminished over the years, the method has found increasing use for site investigations for civil engineering. It is a valuable investigative tool well-suited for shallow surveys, particularly when used in conjunction with the exploratory drill.

Significant advances in refraction-seismograph instrumentation have not occurred to the same extent that they have in the development of the sophisticated reflection equipment used for oil exploration. Solid state electronics have improved the portability of engineering type refraction instruments, but they operate fundamentally in the same way they did 40 years ago. The basic field practices and methods of interpreting the data have not changed with time, although specialized interpretational techniques have been proposed and developed for some difficult cases.

The conduct of refraction surveys and the interpretation of the data are well-established and reasonably straight-forward, although they are not invariant. The user can change the field layout of his equipment and apply judgment and imagination in his handling of the raw data. In common with other indirect methods of subsurface exploration, there

are no rigid, inflexible approaches to making sense of the data, nor are there any handbooks that infallibly direct the engineer, geologist, or geophysicist to the correct answer. The general case will require thought and care; ambiguities and uncertainties are not uncommon. Some foreknowledge of site conditions and an understanding of what is geologically . plausible will always assist in resolving the raw data into meaningful information.

SCOPE

This report addresses the elements of refraction theory, the basic methods of interpretation, a variety of applications, and some of the limitations. In discussing the theory of the method, it is the intention of this report to progress from the simple to the more realistic, deriving the formulas and procedures for interpretation as we go along. The treatment is far from exhaustive, but suitable references to the literature are included for those who wish to pursue a specific aspect of the method.

Theory

FUNDAMENTALS

This section will review the principles of seismic refraction theory and will develop those methods of interpretation that have the widest use. There are many textbooks on geophysics that discuss the principles and applications of refraction surveys; however, most of them are oriented towards exploration for oil and give only passing attention to detailed shallow investigations. Numerous journal articles treat the solution of specific interpretation problems but only a few of these articles have broad application. Much of the following material will be familiar to engineers and geologists who have taken a first course in geophysics or who have acquired first-hand experience with refraction surveys. The elements are presented for those who have had no previous exposure or who desire a review of background material.

Before going into detail, it is appropriate to present a synopsis of refraction exploration so that the factors discussed later can be viewed with some sense of perspective.

The refraction method consists of measuring (at known points along the surface of the ground) the travel times of compressional waves generated by an impulsive energy source. The energy source is usually a small explosive charge and the energy is detected, amplified, and recorded by special equipment designed for this purpose. The instant of the explosion, or "zero-time," is recorded on the record of arriving pulses. The raw data, therefore, consists of travel times and distances, and this time-distance information is then manipulated to convert it into the format of velocity variations with depth. The interpretation of this raw data will be developed as we go along.

The process is schematically illustrated in Fig. 1. All measurements are made at the surface of the ground, and the subsurface structure is inferred from

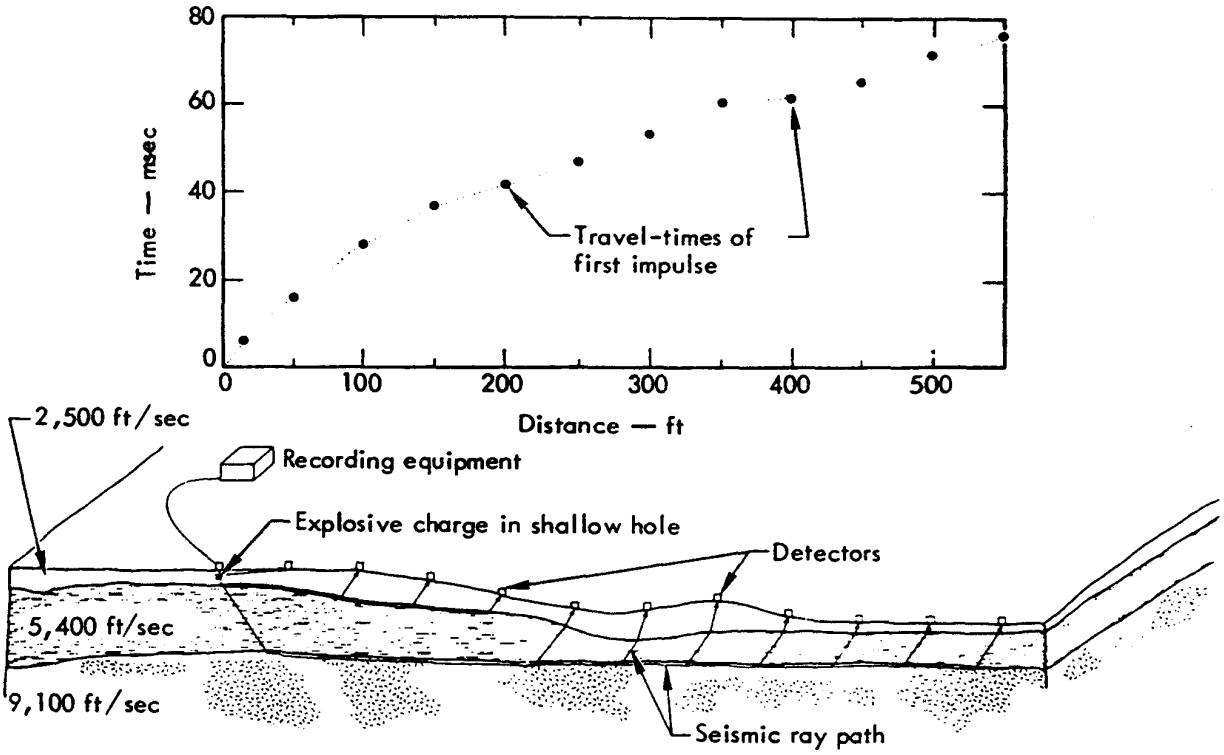

Fig. 1. Schematic of seismic refraction survey.

interpretation methods based on the laws of energy propagation.

The propagation of seismic energy through subsurface layers is described by essentially the same rules that govern the propagation of light rays through transparent media. The refraction or angular deviation that a light ray or seismic pulse undergoes when passing from one material to another depends upon the ratio of the transmission velocities of the two materials. The fundamental law that describes the refraction of light rays is Snell's Law, and this, together with the phenomenon of "critical incidence," is the physical foundation of seismic refraction surveys.

Snell's Law and critical incidence are illustrated in Fig. 2a, which shows a medium with a velocity V_1, underlain by a medium with a higher velocity V_2. Figure 2b is a plot of the relative amplitudes of the pulses transmitted into, and reflected from, the higher speed material.* Until the critical angle of incidence is reached, almost all of the compressional energy is transmitted (refracted) into the higher velocity medium. When the critical angle is exceeded, the energy is almost totally reflected and no energy is refracted into the high-speed layer. Note

*It may seem anomalous in Fig. 2b that the sum of the amplitudes of the reflected and refracted pulses is greater than that of the incident wave (i.e., greater than 1.0). However, the energy of a pulse is proportional to the square of its amplitude, and the sum of the energies of the reflected and refracted waves is equal to the energy of the incident wave.

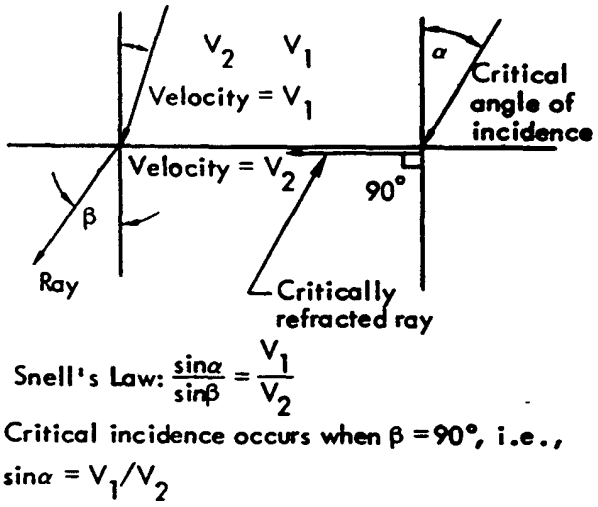

Fig. 2a. Snell's Law and refraction of ray transmitted across boundary between two media with different velocities ($V_2 = 2V_1$).

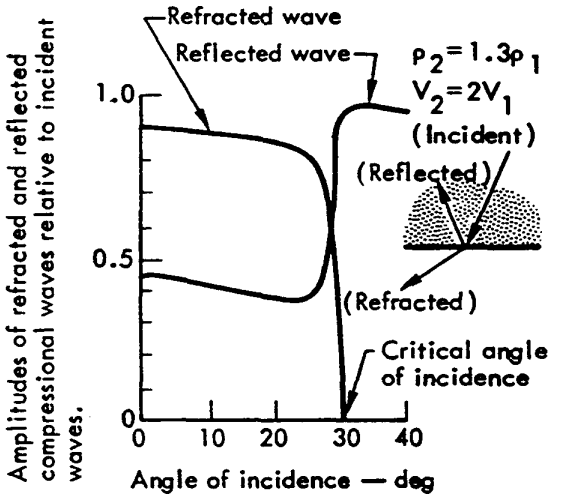

Fig. 2b. Amplitudes of reflected and refracted compressional waves relative to incident waves as a function of angle of incidence.

that we are dealing only with compressional waves and ignoring shear energy and the transformation of a portion of the compressional wave into a shear wave that can occur at boundaries.

The particular case of the critical angle of incidence is fundamental to the derivation of the formulas for refraction exploration. Although the exact mathematical and physical description of what occurs when a ray is incident at the critical angle is complex, it is entirely adequate to assume that the critically refracted ray travels along the boundary between the two media at the higher of the two velocities. Further, as the critically refracted ray travels along the boundary, it continually generates seismic waves in the lower-velocity (upper) layer that depart from the boundary at the angle of critical incidence. In the literature these waves are frequently referred to as head waves. If the velocities of the layers increase with depth, a portion of the energy will eventually be refracted back to the surface where it can be detected.

The following derivations of the refraction equations assume that the subsurface layers possess certain characteristics: each layer within a stratigraphic sequence is isotropic with regard to its propagation velocity, ray paths are made up of straight-line segments, and each layer has a higher velocity than the overlying one. These are entirely reasonable assumptions and relatively few actual cases will depart from these assumptions. The special case of a velocity reversal (i.e., a layer having a lower velocity than the one which overlies it) will be discussed later. The special situation in which velocity increases continuously (vs incrementally) with depth will also be discussed briefly later in the report.

We begin with the simplest of all cases: two layers with plane and parallel boundaries as illustrated in Fig. 3. A small explosive charge is detonated in a shallow hole at A and the energy is

detected by a set of detectors laid out in a straight line along the surface. The arrival times of the impulses are plotted against the corresponding shot-to-detector distances as shown in Fig. 3. The first few arrival times are those of direct arrivals through the first layer, and the slope of the line through these points, $\Delta T/\Delta X$, is simply the reciprocal of the velocity of that layer; i.e., $1/V_1$. At some distance from the shot, a distance called the critical distance, it takes less time for the energy to travel down to the top of the second layer, refract along the interface at the higher velocity V_2 and travel back up to the surface, than it does for the energy to travel directly through the top layer. The energy that arrives at the detectors beyond the critical distance will plot along a line with a slope of $1/V_2$. The line through these refracted arrivals will not pass through the origin, but rather will project back to the time axis to intersect it at a time called the intercept time. Because both the intercept time and the critical distance are directly dependent upon the velocities of the two materials and the thickness of the top layer, they can be used to determine the depth to the top of the second layer.

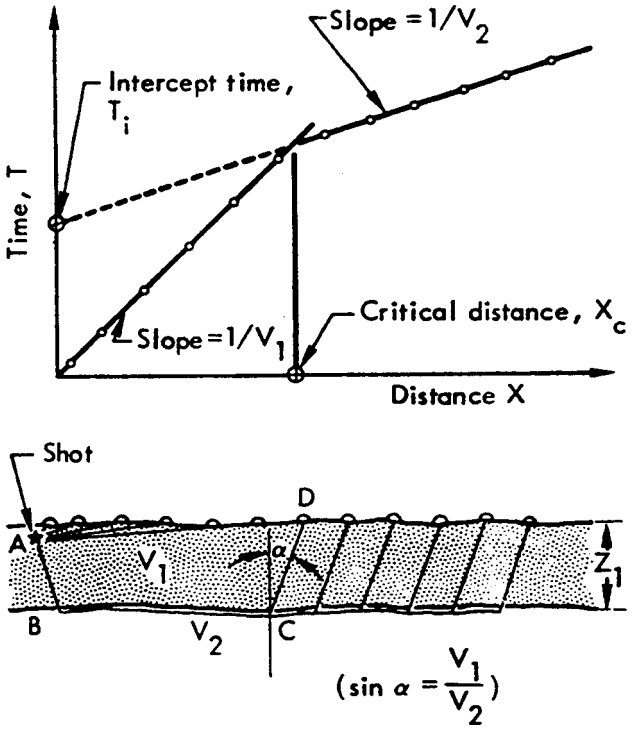

Fig. 3. Simple two-layer case with plane, parallel boundaries and corresponding time-distance curve.

INTERCEPT TIMES

Referring to Fig. 3, let us compute the arrival time of the refracted impulse at a detector. Consider the travel path ABCD:

$$AB = CD = \frac{Z_1}{\cos \alpha}$$

and

$$BC = X - 2Z_1 \tan \alpha,$$

where Z_1 is the thickness of the top layer, and a is the critical angle of incidence. The travel time is therefore given by:

$$T = \frac{AB + CD}{V_1} + \frac{BC}{V_2}$$

$$= \frac{2Z_1}{V_1 \cos \alpha} + \frac{X - 2Z_1 \tan \alpha}{V_2}$$

$$= 2Z_1 \left(\frac{1}{V_1 \cos \alpha} - \frac{\sin \alpha}{V_2 \cos \alpha} \right) + \frac{X}{V_2}$$

$$= 2Z_1 \left(\frac{V_2 - V_1 \sin \alpha}{V_1 V_2 \cos \alpha} \right) + \frac{X}{V_2}.$$

Snell's law defines the critical angle of incidence, a, by:

$$\sin \alpha = \frac{V_1}{V_2}, \qquad (1)$$

and selectively substituting Eq. (1) into the previous equation:

$$T = 2Z_1V_1\left(\frac{\frac{1}{\sin\alpha} - \sin\alpha}{V_1V_2\cos\alpha}\right) + \frac{X}{V_2}$$

$$= 2Z_1V_1\left(\frac{1 - \sin^2\alpha}{V_1V_2\sin\alpha\cos\alpha}\right) + \frac{X}{V_2}$$

$$= \frac{2Z_1\cos^2\alpha}{V_2\sin\alpha\cos\alpha} + \frac{X}{V_2},$$

and substituting V_1 for $V_2\sin\alpha$,

$$T = \frac{2Z_1\cos\alpha}{V_1} + \frac{X}{V_2}$$

If we now let X = 0, then T becomes the intercept time, T_i, and we can rewrite the last expression as:

$$Z_1 = \frac{T_iV_1}{2\cos\alpha},$$

i.e.,

$$Z_1 = \frac{T_iV_1}{2\cos\left(\sin^{-1}V_1/V_2\right)}.^{*} \qquad (2)$$

For the situation we have assumed in Fig. 3, everything on the right-hand side of Eq. (2) can be determined from the time-distance plot; therefore, the depth to the second layer can be computed. The depth of the shot has been ignored in the derivation above, and the true depth to the second layer is determined simply by adding one-half the shot depth to the value of Z_1 computed by Eq. (2).

In the particular example of Fig. 3, the depth computed by Eq. (2) is the depth along the entire seismic line because we stipulated that the layers were plane and parallel.

A very important point to bring out at this time is that all depths determined in refraction surveys are measured normal to the boundary between layers and are not necessarily vertical depths beneath the ground surface.

The intercept-time analysis can be extended to the case of multiple layers; however, only the resulting formulas will be given here because their derivations are redundant and may be found in a number of references. [1,2] Figure 4 schematically illustrates the multiple layer case

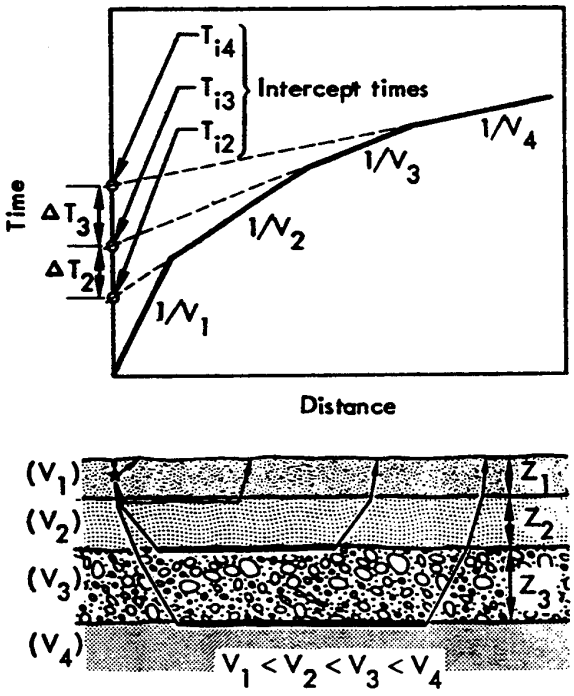

Fig. 4. Schematic of multiple-layer case and corresponding time-distance curve.

*An alternative version of this equation is:

$$Z_1 = \frac{T_iV_1V_2}{2\left(V_2^2 - V_1^2\right)^{1/2}}.$$

and corresponding time-distance plot. Note Mat the intercept times and layer thicknesses have been identified by a subscript corresponding to the number of the layer:

$$Z_1 = \frac{(T_{i2})\, V_1}{2 \cos\left(\sin^{-1} V_1/V_2\right)} + \frac{1}{2} \text{ shot depth} \qquad (3)$$

$$Z_2 = \frac{\left[T_{i3} - T_{i2} \dfrac{\cos\left(\sin^{-1} V_1/V_3\right)}{\cos\left(\sin^{-1} V_1/V_2\right)}\right] V_2}{2 \cos\left(\sin^{-1} V_2/V_3\right)} \qquad (4)$$

$$Z_3 = \left[T_{i4} - T_{i2} \frac{\cos\left(\sin^{-1} V_1/V_4\right)}{\cos\left(\sin^{-1} V_1/V_2\right)} - \frac{2Z_2 \cos\left(\sin^{-1} V_2/V_4\right)}{V_2}\right] V_3 \Big/ 2 \cos\left(\sin^{-1} V_3/V_4\right). \qquad (5)$$

If the velocity contrasts between layers are high enough; say 2 to 1, and only approximate depths are required, then the following formulas can be used:

$$Z_2 = \frac{(\Delta T_2) V_2}{2 \cos\left(\sin^{-1} V_2/V_3\right)} \qquad (6)$$

$$Z_3 = \frac{(\Delta T_3) V_3}{2 \cos\left(\sin^{-1} V_3/V_4\right)} \qquad (7)$$

where ΔT_2 and ΔT_3; are as indicated in Fig. 4. Equations (6) and (7) will give thicknesses that are greater than actual, and it is suggested that thicknesses initially be computed both ways to learn whether the error is significant in a particular situation.

CRITICAL DISTANCE

The critical-distance method for determining depth will receive only brief attention here because it is analagous to the intercept-time method, and offers no advantages significant enough to warrant further detail. Its primary application is to compute the depth of the first layer and to estimate the length of the seismic line required for a particular exploration task.

The critical distance is the distance from the shot point to the point at which the refracted energy arrives at the same time as the energy traveling directly through the top layer. The critical distance (X_c) is illustrated in Fig. 3; it is the breakpoint in the graph of arrival times.*

By an approach similar to the one used in deriving the intercept-time formulas, it can be shown that the depth of the first layer is given by:

$$Z_1 = \frac{X_c}{2} \frac{(1 - V_1/V_2)}{\cos\left(\sin^{-1} V_1/V_2\right)} \qquad (8)$$

where X_c is the critical distance.

---

*There is, of course, a critical distance for refractions from each layer in a multilayer case; we are concerned here only with the first breakpoint.

Equation (8) can be used to construct a graph showing the length of a seismic line (relative to the depth of the first layer) required to detect refractions from the underlying layer, as a function of velocity ratios. Figure 5 is a graph of Eq. (8), which can be of use in planning a seismic survey if velocity ratios are assumed. The graph also assists in giving a sense of perspective to the effect of velocity contrasts. For example, assume that there is about 15 ft of overburden with a velocity of 2, 500 ft/sec, and that it is underlain by a shale with a velocity of about 5,500 ft/sec. How long should the seismic line be to insure adequate coverage for mapping the overburden thickness? The velocity ratio, V_2/V_1 , is 2.2 so that X_c/Z_1 is approximately 3.25, which means that the critical distance will be about 50 ft. The seismic spread should be at least three times this distance; therefore, a seismic line 150 to 200 ft long would be satisfactory.

DIPPING LAYERS

We will now briefly consider the existence of a dipping interface, the concept of apparent velocities, and their effect on depth computations.

The equations derived above require knowledge of the "true" velocities of the layers. If the boundaries between interfaces are nonparallel (i.e., if there are dipping interfaces), a plot of arrival times vs distance will give only apparent velocities for the refracting layers, and the use of these apparent velocities will result in erroneous depths: The case of a dipping boundary and its effect on travel-time plots is illustrated in Fig. 6. Figure 6 also introduces the idea of

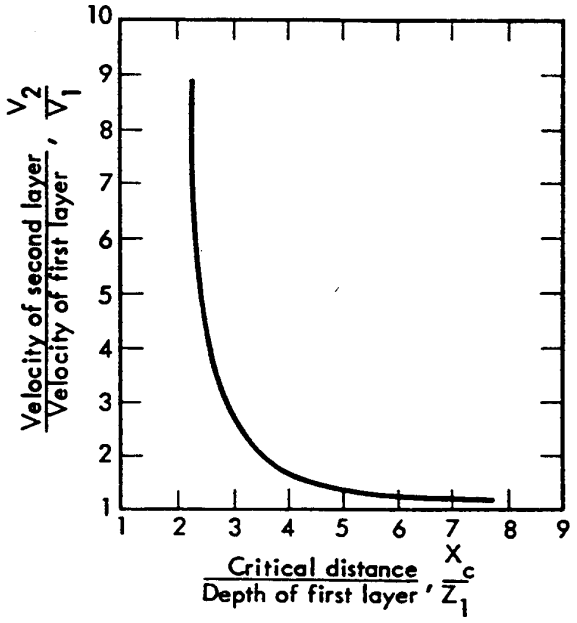

Fig. 5. Plot of ratio of critical distance to depth of first layer as a function of velocity contrast.

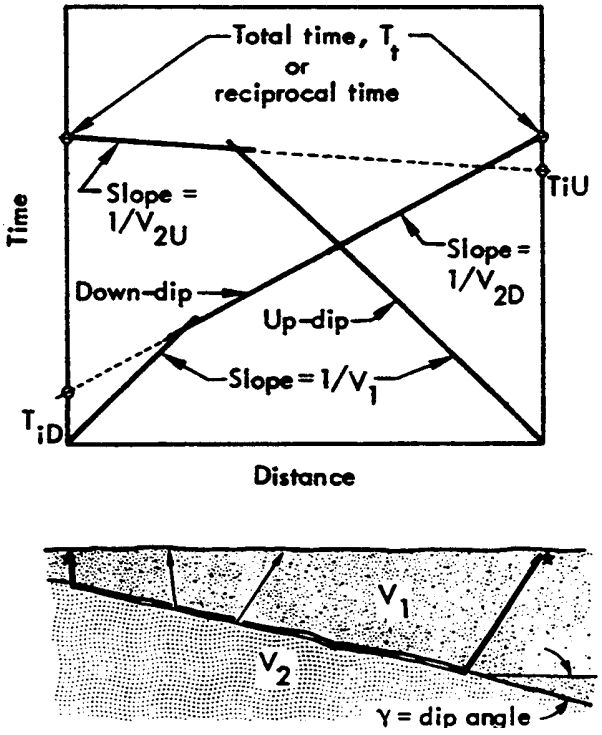

Fig. 6. Example of dipping interface and concepts of reverse shooting and "apparent velocity:'

"reverse shooting" of which should always be applied in refraction surveys. Reverse shooting simply means firing a shot at both ends of the seismic line so that arrival times at each detector are measured from both directions.

It is evident from Fig. 6 that the apparent velocity of the refracting layer, as determined from the time-distance plot, depends upon whether the shot is fired at the up-dip or the down-dip end of the seismic line, and that a depth determined on the basis of only one shot will be valid only at one point along the line. Unless the dip angle is known, reverse shooting is required to determine the true value of V_2.

If the apparent velocity of the refractor as observed from the down-dip shot is V_{2D}, then from Snell's Law:

$$V_{2D} = V_1 / \sin (\alpha + \gamma),$$

where γ is the dip angle of the interface relative to the surface and α is the critical angle of incidence. Similarly, the apparent velocity, V_{2U}, observed for the shot in the up-dip direction is given by:

$$V_{2U} = V_1 / \sin (\alpha - \gamma).$$

We can rearrange the two relationships above to obtain:

$$\alpha + \gamma = \sin^{-1} \left(\frac{V_1}{V_{2D}} \right)$$

$$\alpha - \gamma = \sin^{-1} \left(\frac{V_1}{V_{2U}} \right)$$

from which the dip angle can be determined:

$$\gamma = \frac{1}{2} \left[\sin^{-1} \left(\frac{V_1}{V_{2D}} \right) - \sin^{-1} \left(\frac{V_1}{V_{2U}} \right) \right]. \qquad (9)$$

The true value of V_2 is not the arithmetic average of V_{2U} and V_{2D}, but is instead the harmonic mean multiplied by the cosine of the dip angle:

$$V_2 = \frac{2V_{2U}V_{2D}}{V_{2U} + V_{2D}} \cos \gamma. \qquad (10)$$

Other methods of determining true velocities will be discussed later.

As an example of the degree to which a dipping interface can affect observed velocities on a time-distance plot, consider the case of a 2,000-ft/sec material overlying a 5,000-ft/sec material with their interface dipping 10 deg relative to the surface. The following refractor velocities would be observed:

Up-dip (V2U):	8,515 ft/sec
Down-dip (V2D):	3,615 ft/sec
Arithmetic average:	6,065 ft/sec
Harmonic mean:	5,075 ft/sec
Harmonic mean X Cos γ:	5,000 ft/sec = true velocity

The harmonic mean is generally accurate enough for computations; i.e., it is not usually necessary to compute the dip angle unless it is of interest in itself.

Depths are always computed using true velocities. The use of apparent velocities may result in significant errors.

DELAY TIMES

Previously, it was pointed out that true refractor velocities cannot be determined by firing a shot at only one end of

a seismic line, but that such velocities can be determined if arrival times are recorded from both ends. Further, a depth computed from an intercept time actually represents the depth of the refracting surface projected back to the shot point. The reversed profile, however, offers a significant advantage in that the true velocities and the thicknesses of layers can be computed on a much more detailed basis by means of delay times. Under ideal circumstances, depths can be determined beneath each geophone to allow mapping of irregular and dipping boundaries.

The meaning of the term "delay time" is illustrated by reference to Fig. 7 in which the delay time is defined at the shot point and at the detector.* The delay time is the difference between the time actually spent by the pulse traveling on its upward or downward path through the upper layer, and the time it would have spent traveling, at the refractor velocity, along the normal projection of this path on the interface. Although the definition of the delay time may at first appear to be cumbersome, its meaning and application will become clearer as we progress. Consider the pulse traveling up to the detector in Fig. 7 for which the delay time has been defined as:

$$\text{Delay time at detector} = \Delta T_D = \frac{CD}{V_1} - \frac{CD'}{V_2}$$

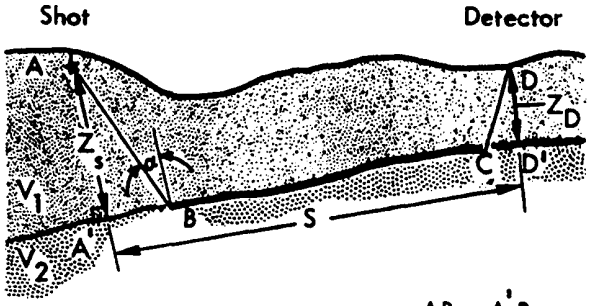

$$\text{Delay time at shot point} = \Delta T_S = \frac{AB}{V_1} - \frac{A'B}{V_2}$$

$$\text{Delay time at detector} = \Delta T_D = \frac{CD}{V_1} - \frac{CD'}{V_2}$$

Fig. 7. Definition of delay time.

$$\Delta T_D = \frac{Z_D}{V_1 \cos \alpha} - \frac{Z_D \tan \alpha}{V_2}$$

$$= Z_D \left(\frac{1}{V_1 \cos \alpha} - \frac{\sin \alpha}{V_2 \cos \alpha} \right)$$

and because $\sin \alpha = V_1/V_2$

$$\Delta T_D = Z_D \left(\frac{1}{V_1 \cos \alpha} - \frac{\sin^2 \alpha}{V_1 \cos \alpha} \right),$$

and because $\sin^2 \alpha + \cos^2 \alpha = 1$,

$$\Delta T_D = \frac{Z_D \cos \alpha}{V_1}$$

$$= \frac{Z_D \cos \left(\sin^{-1} V_1/V_2 \right)}{V_1}, \qquad (11)$$

so that

$$Z_D = \frac{\Delta T_D V_1}{\cos \left(\sin^{-1} V_1/V_2 \right)}. \qquad (12)$$

The equivalence between a delay time and an intercept time is apparent when Eq. (12) is compared to the intercept-time

---

* Although the distinction is not important in the context of this report, the delay time" is referred to as the timedepth, in some of the literature. Strictly speaking, the term delay time implies that the refractor surface is horizontal; in this report depths are measured normal to the refractor surface, regardless of its disposition.

formula, Eq. (2). A delay time can be thought of as being analagous to the time taken by a pulse to travel upward or downward through a layer. from one interface to the next. It is evident that if the value of the delay time, ΔT_D, at a particular detector can be determined, then the depth beneath the detector can be computed.

Before discussing the method by which delay times are determined, we will consider the path of the refracted pulse, from shot to detector, which is shown in Fig. 7. The total delay time is, by definition:

$$\Delta T_{SD} = T_t - \frac{S}{V_2},$$

where T_t is the observed total travel time from shot to detector. It can be shown that the total delay time is the sum of the delay times at the shot and at the detector; i.e.,

$$\Delta T_{SD} = \Delta T_S + \Delta T_D,$$

and by combining these two expressions we obtain the following equation for the delay time beneath the detector:

$$\Delta T_D = T_t - \frac{S}{V_2} - \Delta T_S. \qquad (13)$$

Consequently, if the delay time at the shot (ΔT_S) were known, ΔT_D and the depth beneath the geophone could be calculated.

If the depth of the refractor beneath the shot and the velocities of the layers are known beforehand, then ΔT_S can be calculated, and the arrival time from only one end of the line would be sufficient to determine the delay time and depth beneath the geophone. Although the depth beneath the shot and the velocities are not generally known beforehand, the delay time beneath the geophone can nevertheless be determined by firing shots at both ends of the line.

The reversed seismic line shown in Figure 8 will be used to illustrate the method of delay times. Figure 8 shows the arrival times at the geophones from shots at both ends of a seismic line. The total travel time from one end of the line to the other (sometimes called the "reciprocal" time)[3] has been designated T_t and should be the same for both shots.* The arrival times at one of the (arbitrarily selected) geophones from the two shots, SP_1 and SP_2, have been designated T_{D1}

* If the shot depths are equal.

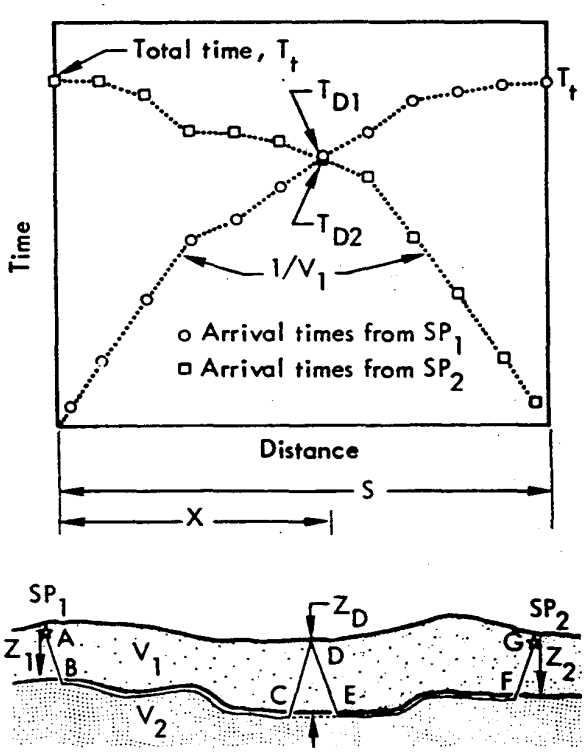

Fig. 8. Schematic of reversed seismic line and delay-time method of depth determination.

and T_{D2}, respectively. Remembering that the objective is to find the delay time, ΔT_D, at the geophone, consider the following. From Eq. (13) we can write each arrival time in terms of the component delay times:

$$T_{D1} = \Delta T_{S1} + \Delta T_D + \frac{X}{V_2}$$

and

$$T_{D2} = \Delta T_{S2} + \Delta T_D + \frac{S - X}{V_2};$$

therefore, $T_{D1} + T_{D2} = \Delta T_{S1} + \Delta T_{S2} + 2\Delta T_D + S/V_2$, where ΔT_S is the delay time at a shot point. Similarly the total time can be expressed in terms of delay times:

$$T_t = \Delta T_{S1} + \Delta T_{S2} + \frac{S}{V_2};$$

therefore,

$$T_{D1} + T_{D2} = 2\Delta T_D + T_t;$$

i.e.,

$$\Delta T_D = \frac{1}{2}\ (T_{D1} + T_{D2} - T_t). \qquad (14)$$

Note that the delay time beneath the geophone is determined by subtracting the total time from the sum of the two arrival times, and taking half the result. The depth beneath the geophone to the top of the refractor is then calculated by Eq. (12):

$$Z_D = \frac{\Delta T_D V_1}{\cos\left(\sin^{-1} V_1/V_2\right)}.$$

It is important to keep in mind that TV the total time that is subtracted from the sum of the two arrival times in Eq. (14), must be the arrival time of a pulse refracted from the same layer from which the two other arrivals were refracted. The total time cannot be the arrival time of a pulse refracted from a deeper layer.

In the event that the derivation of Eq. (14) by means of something called a delay time appears circuitous and indirect, the following analysis, also based on Fig. 8, is presented as an alternative:

$$T_t = \frac{AB}{V_1} + \frac{BCEF}{V_2} + \frac{FG}{V_1}$$

$$= \frac{Z_1}{V_1 \cos\alpha} + \frac{S - Z_1 \tan\alpha - Z_2 \tan\alpha}{V_2} + \frac{Z_2}{V_1 \cos\alpha}.$$

$$T_{D1} = \frac{AB}{V_1} + \frac{BC}{V_2} + \frac{CD}{V_1}$$

$$= \frac{Z_1}{V_1 \cos\alpha} + \frac{X - Z_1 \tan\alpha - Z_D \tan\alpha}{V_2} + \frac{Z_D}{V_1 \cos\alpha}.$$

$$T_{D2} = \frac{FG}{V_1} + \frac{EF}{V_2} + \frac{DE}{V_1}$$

$$= \frac{Z_2}{V_1 \cos\alpha} + \frac{(S - X) - Z_2 \tan\alpha - Z_D \tan\alpha}{V_2} + \frac{Z_D}{V_1 \cos\alpha}.$$

Combining these:

$$T_{D1} + T_{D2} - T_t = \frac{2Z_D}{V_1 \cos \alpha} - \frac{2Z_D \tan \alpha}{V_2}$$

$$= 2Z_D \left(\frac{1}{V_1 \cos \alpha} - \frac{\sin \alpha}{V_2 \cos \alpha} \right),$$

and because $V_2 = V_1 / \sin \alpha$,

$$T_{D1} + T_{D2} - T_t = \frac{2Z_D}{V_1} \left(\frac{1 - \sin^2 \alpha}{\cos \alpha} \right)$$

$$= \frac{2Z_D \cos \alpha}{V_1};$$

therefore,

$$Z_D = \frac{1}{2} \frac{(T_{D1} + T_{D2} - T_t) V_1}{\cos \alpha},$$

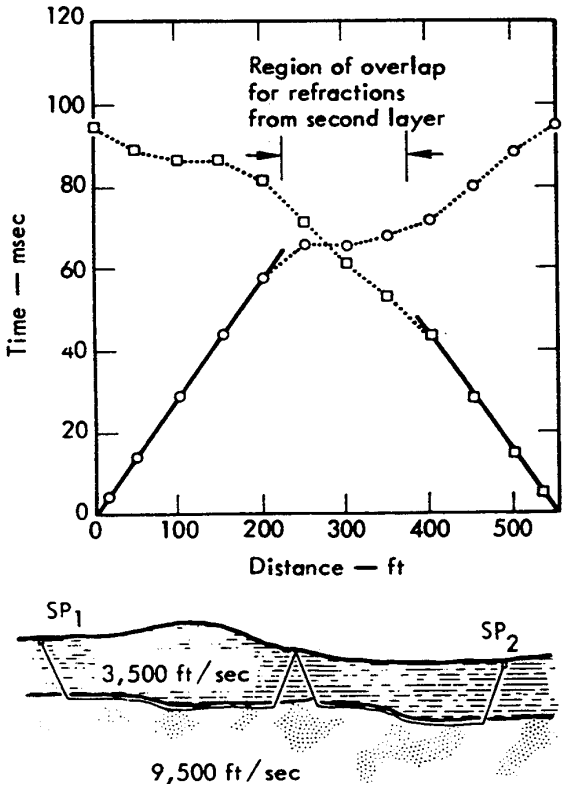

Fig. 9a. Reversed seismic profile in which refracted arrivals from both ends are recorded at only three detectors.

or, as before,

$$Z_D = \frac{\Delta T_D V_1}{\cos \left(\sin^{-1} V_1 / V_2 \right)}.$$

The first derivation, which explicitly uses a delay time, is the one commonly found in the literature.

Before extending the delay-time method to a case in which there are more than two layers, it is important to note that the method can be applied only where there is "overlap" between arrivals refracted from the same layer. In other words, the actual length of the seismic line should be sufficient to insure overlapping of the refracted arrivals. This point is illustrated in Fig. 9a, which

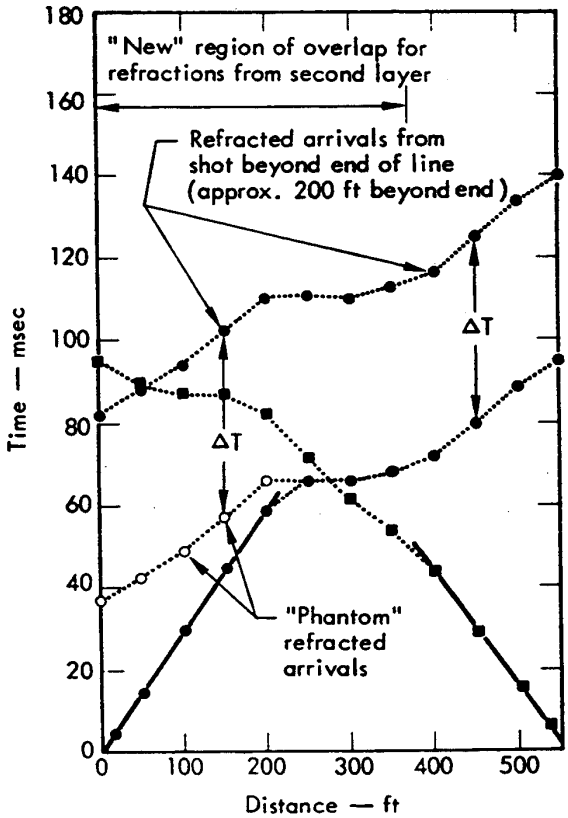

Fig. 9b. Increasing overlap of refracted arrivals for situation in Fig. 9a by firing shot beyond end of line and plotting phantom arrivals.

shows the reversed time-distance curves synthesized for a two-layer case. Although not immediately obvious from a look at the time-distances curves, only three of the detectors near the center of the line recorded refractions from both directions. Consequently, delay times can be determined only for these three detectors. If the seismic line had been longer more of the refracted arrivals would have overlapped, and more delay times could be determined.

If the lack of overlap is noted in the field by reducing and plotting the data immediately after the shots. it is often possible to partially remedy the situation by firing additional shots off one or both ends of the line (i.e., beyond the end of the seismic cable) in line with the detector array. The arrival times from a beyond-the-end shot are used to extrapolate the first set of refracted arrivals back towards the shot point.* This technique is referred to as "phantoming" and is illustrated in Fig. 9b, which shows the same data as Fig. 9a but with the addition of a beyond-the-end shot.

If the plot of arrival times from the beyond-the-end shot parallels the arrival times from the end shot, they represent refractions from the same layer. This is the case in Fig. 9b, in which the difference in arrival times between refracted arrivals from both the end and the beyond-the-end shots is a constant, AT. Figure 9b shows how the refracted arrivals from the end shot are extrapolated back towards the shot point by reducing the beyond-the-end arrival times by ΔT to produce the phantom arrivals at distances less than the critical distance. These phantom arrivals can then be used to determine delay times over the region shown in Fig. 9b. An additional shot could also be fired beyond the other end of the line to allow delay times to be determined over the entire spread, permitting the depth to the refractor to be computed beneath every detector. If there is a shot at the center of a seismic line, the shots placed at the ends of the cable are, in effect, beyond-the-end shots for the opposite half of the line. If the arrival times from a beyond-the-end shot do not parallel the times from the end shot, there is a third, deeper layer present; this situation is discussed below.

In general, the interpreter is cautioned to try to assure himself that the two arrival times that he is using to compute a delay time represent refractions from the same layer; otherwise he will be “Mixing apples and oranges.” Verifying the stratigraphic origin of an arrival is not always easy.

The delay-time method is not limited to the simple two-layer case. Ideally. a delay time would be computed beneath each geophone for each layer in a sequence, but this is almost never possible. Figure 10 illustrates a very common situation in refraction investigations. Note that there are three layers and that the travel paths of the first arrivals are shown on the drawing. Examination of Fig. 10 will show that only two of the detectors (at Stations 250 and 300) recorded refractions from the third layer from both of the end shots. There is obviously

---

* We are assuming, of course, that the arrivals from the beyond-the-end shot have been refracted from the layer from which the first set of arrivals was refracted.

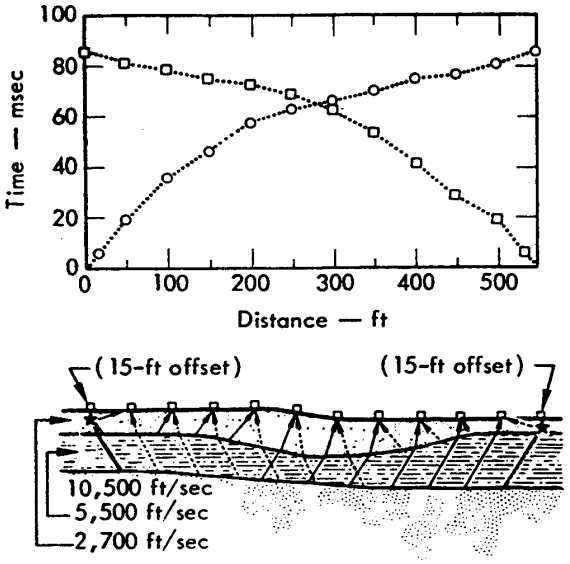

Fig. 10. Three-layer case showing travel paths of first arrivals and corresponding time-distance curves.

no overlap of refractions from the second layer. The two delay times that can be determined at Stations, 250 and 300 will be the sum of the delay times for the first and second layers. The delay time in the first (top) layer must be subtracted from the total delay time before the thickness of the second layer can be computed. However, with only the information shown in Fig. 10, we have no way of determining the actual delay time for the first layer.

If we had only the arrival times from the two end shots as shown in Fig. 10, our only recourse would be to compute the thickness of the first layer at each end of the line by using the intercept-time formula, and to interpolate linearly these two values of depth across the length of the line. The interpolated depths of the first layer could be converted to delay times at Stations 250 and 300 by Eq. (11). and then subtracted from the total delay times determined at these two detectors. The result would be values of delay times for the second layer at these two stations, and the thickness of the second layer would be interpreted as:

$$Z_2 = \frac{(\Delta T_{12} - \Delta T_1)\, V_2}{\cos\left(\sin^{-1} V_2/V_3\right)}, \qquad (15)$$

where ΔT_{12} is the combined delay time for the first and second layers, and ΔT_1 is the delay time for the first layer computed from interpolated values of depth and Eq. (11).

Inspection of Fig. 10 will show that the above procedure will lead to some very wrong answers. The first layer thickens appreciably in the middle of the spread, but there is no way of knowing this if shots are fired only at the ends of the spread. The thickness of the second layer would be considerably overestimated because the thickness of the first layer was underestimated; i.e., an insufficient amount of time would be subtracted from the total delay times at Stations 250 and 300. Computing depths on the basis of the intercept times of the third-layer refractions would result in the same errors.

The situation described above and depicted in Fig. 10 was chosen to illustrate the merit of firing intermediate shots along the length of a seismic line. Intermediate shot points will result in better control of first-layer depths and velocities; fewer assumptions are required to interpret the raw data.

Figure 11 is the same as Fig. 10, except that a shot in the middle of the spread has been added. An intercept

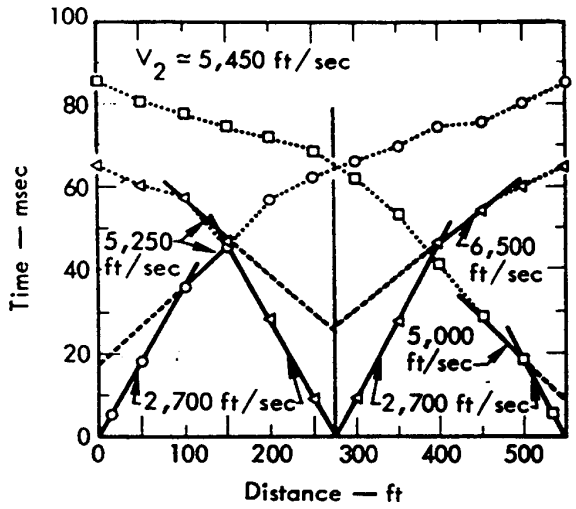

Fig. 11. Same time-distance curves as shown in Fig. 10 but with addition of shot at center of seismic line.

time can now be obtained at the center as well as the ends of the line, and we also have a check on the first-layer velocity at the center.

It would be apparent from the intercept times in Fig. 11 that the 2,700-ft/sec first-layer is thicker near the center of the line than at the ends; consequently, a much more accurate appraisal of the second layer's thickness could now be made. Additional intermediate shots would help resolve the first layer in greater detail, and eventually permit more detailed mapping of the second layer.

The apparent velocities of the second layer shown in Fig. 11 may appear to vary considerably. The velocities on the right-hand portion are up-dip and down-dip dip velocities with a harmonic mean of about 5,650 ft/sec. The overall average for V_2 is about 5,450 ft/sec, very close to the nominal value of 5,500 ft/sec. The scatter of values about the nominal value is typical of the accuracy that can be expected in refraction surveys.

In the hypothetical case being considered (Fig. 11) we can obtain enough detail about the top layer by means of intermediate shots. In this particular example there is not enough overlap of refractions from the top of the second layer to compute first-layer thicknesses by the delay-time method. This will generally be the case for multilayer situations. If this were a typical engineering survey our interest would probably be directed toward mapping the top of the high-speed layer (10,500 ft/sec). How do we obtain more information? With the data in Fig. 11 we could compute the depth to the top of the third layer at three locations; i.e., at the center and ends of the line. A beyond-the-end shot is required for more detail.

The arrival times from a shot located beyond the end of the line are shown in Fig. 12. These times were used to generate phantom refracted arrivals by the technique demonstrated in Fig. 9, and delay times were then computed from the overlap of actual and phantom arrival times from Station 250 to Station 550. These delay times are the sum of the delay times in the first and second layer. We now introduce a new technique for using these delay times to extract more information from the data.

If the delay times in Fig. 12 are subtracted from the corresponding arrival times and the differences plotted, we have, in effect, a new time-distance curve that is equivalent to placing the shot and detectors at the top of the third layer. The reduced arrival times should plot with a reciprocal slope equal to the

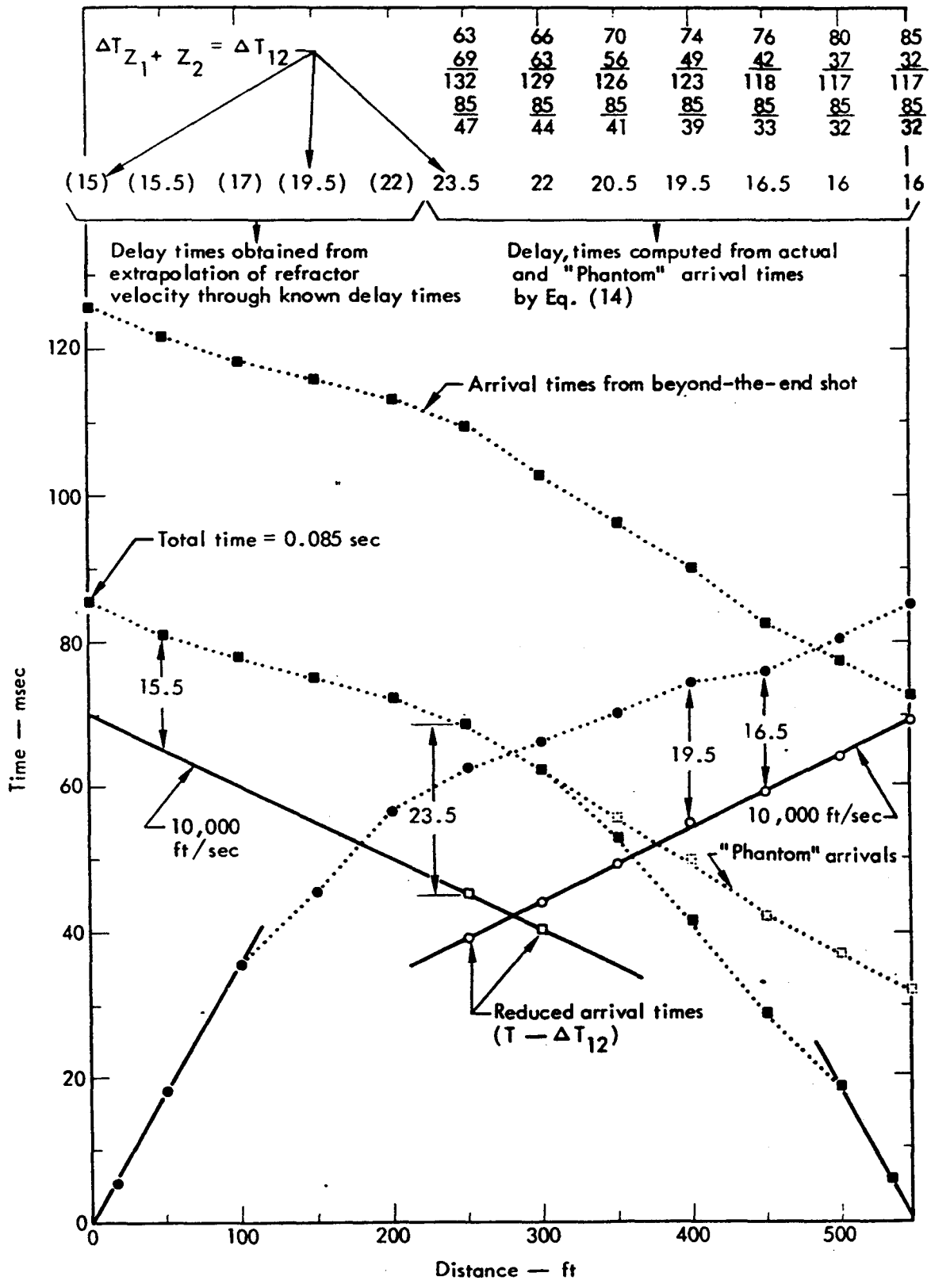

Fig. 12. Same time-distance curves as shown in Fig. 10 but with addition of beyond-the-end shot (center shot has been omitted for sake of clarity).

true velocity of the refracting horizon; i.e., the third layer. This operation has been performed for the detectors at Stations 250 to 550 in Fig. 12, and we see that the reciprocal slope is 10,000 ft/sec, in reasonable agreement with the nominal velocity of 10,500 ft/sec shown in the cross section in Fig. 10. This is a very useful method of determining true refractor velocities. Further, we can draw a line with this same slope through the two reduced arrival times (at Stations 250 and 300) for the reverse shot. Delay times for the detectors at Stations 0 to 200 are then read directly as the difference between the arrival times and the extrapolated line having a reciprocal slope of 10,000 ft/sec. This operation is also illustrated in Fig. 12.

At this point we have total delay times for the first and second layers at each detector on the line. We can determine . the thickness of the first layer by means of intermediate shots and the intercept-time method, interpolate these depths over the full spread to obtain corresponding first-layer delay times at each detector,* and subtract these first-layer times from the total to give us second-layer delay times at each detector.

As a consequence of firing a few intermediate shots along the line and a shot beyond the end, we have been able to arrive at a reasonably detailed interpretation of the subsurface structure. This is in contrast to the very erroneous picture of the subsurface that would result from an interpretation based only on the shots at the ends of the seismic line. Further, we have a reasonable value for the true velocity of the refractor.

The techniques outlined above call be extended to more than three layers, but the difficulties increase, and there is a loss of accuracy and resolution as the number of discrete layers increases.

The foregoing example demonstrated that true velocities could be determined by subtracting delay times from arrival times and plotting the reduced arrival times. There is another method of determining true velocities that is frequently of great value, particularly for determining whether lateral variations of velocity exist along a refracting horizon. This method will be discussed next.

In the alternate derivation of the delay-time formula given earlier, the arrival time of a refraction at a given detector from a shot at the end of the line was:

$$T_{D1} = \frac{Z_1}{V_1 \cos \alpha} + \frac{X - Z_1 \tan \alpha - Z_D \tan \alpha}{V_2} + \frac{Z_D}{V_1 \cos \alpha},$$

and the arrival time at the same geophone from a shot at the opposite end of the seismic line was:

$$T_{D2} = \frac{Z_2}{V_1 \cos \alpha} + \frac{(S - X) - Z_2 \tan \alpha - Z_D \tan \alpha}{V_2} + \frac{Z_D}{V_1 \cos \alpha},$$

* If the shot depths are relatively shallow, say a few feet, half intercept times will be nearly equal to the delay times, and can be interpolated directly.

where Z_1 and Z_2 are depths to the refracting horizon beneath the shot points and Z_D is the depth beneath the detector. The difference in arrival times will be:

$$(T_{D1} - T_{D2}) = \frac{Z_1 - Z_2}{V_1 \cos \alpha} + \frac{2X}{V_2} - \frac{S}{V_2} + \frac{Z_2 \tan \alpha - Z_1 \tan \alpha}{V_2}.$$

For a given seismic line, the only variable term on the right-hand side of the above equation is the second one; therefore:

$$(T_{D1} - T_{D2}) = \text{constant} + \frac{2X}{V_2}. \quad (16)$$

It follows that differences in arrival times plotted against distance, X, will form a line the reciprocal slope of which is half the velocity of the refractor. The method is illustrated in Fig. 13 where arrival-time differences for a three-layer case have been plotted above and below an arbitrary reference line. The arrival times being differenced must represent arrivals from the same refractor. The method is frequently useful for determining whether the arrivals have been refracted from the same layer. A deviation of the points from a straight line may indicate either that there exists a lateral variation of the refractor velocity, or that the times being differenced represent arrivals refracted from two different layers. The latter is the case in Fig. 13.

Problems, Limitations, and Additional Applications

THE BLIND ZONE AND VELOCITY REVERSALS

The following material will be concerned with problems that constitute important limitations to the method, particularly from an engineering geology standpoint. The two major potential problem areas in refraction surveys are the phenomenon of a “blind zone” and the effect of a velocity reversal.

The term blind zone refers to the possible existence of a hidden layer, i.e., the inability of the refraction seismograph to discern the existence of certain beds or layers because of insufficient velocity contrast or thickness. This inability cannot be remedied by any change in the layout of the geophones, and it is probably the greatest drawback of the seismic refraction method. In most cases the blind zone will lie between the surface and a high-speed layer.

An example of this type of problem is taken directly from Soske.[4] Figure 14 from Soske[4] depicts an example of a three-layer case with the layers having good velocity contrasts. However, Fig. 14 shows the minimum thickness of the intermediate 8,500-ft/sec layer that would have to exist before its presence could be detected by first arrivals, regardless of the geophone layout. It will be noted that there is no indication of the 8,500-ft/sec layer on the time-distance curve in Fig. 14.

It would be necessary that the intermediate 8, 500-ft/sec layer in Fig. 14 be at least 70 ft thick in order that refractions from it be recorded as first arrivals. It may seem puzzling that the

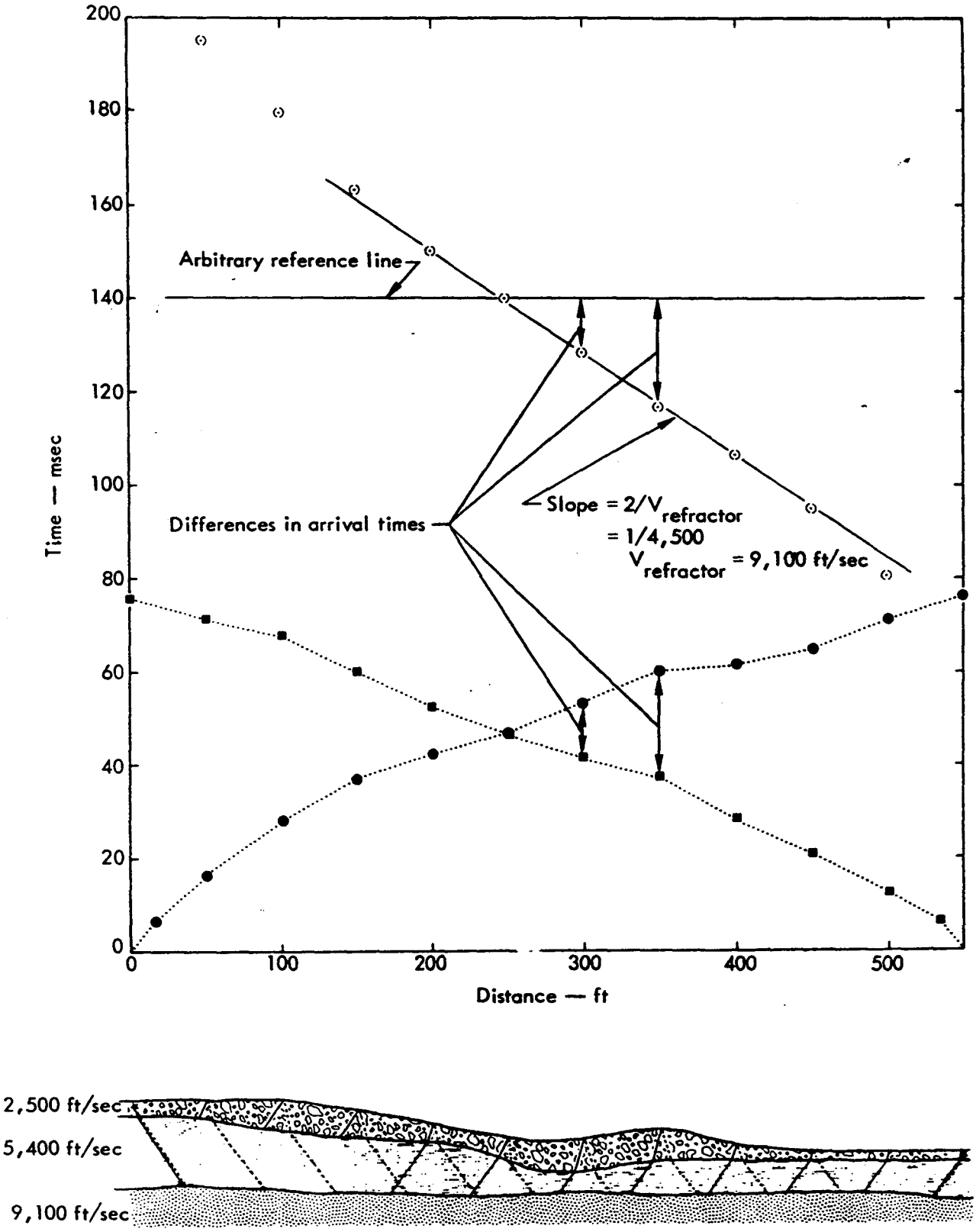

Fig. 13. Method of determining true velocity of refractor by plotting differences of arrival times.

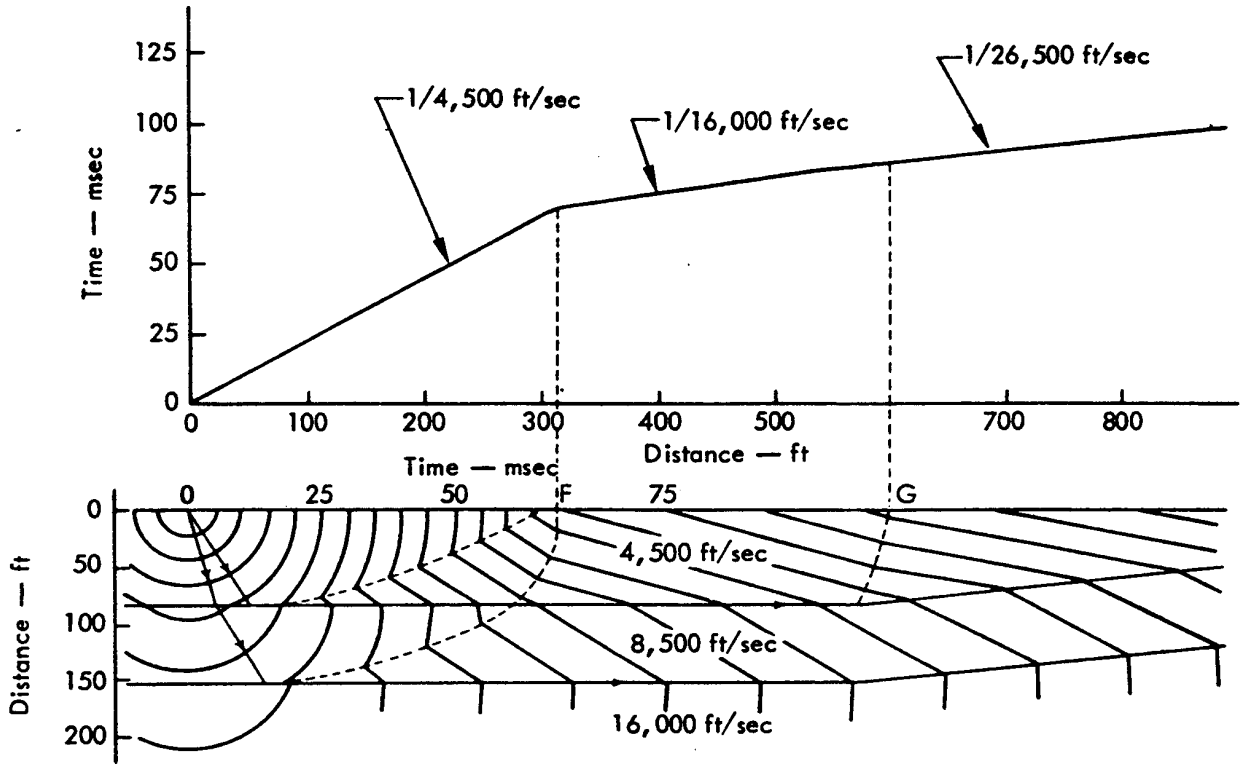

Fig. 14. Wave-front diagram and maximum "undetectable" thickness of "blind zone" (taken from Fig. 4, p. 326 of Soske[4] - used with permission).

8, 500-ft/sec layer be as thick as 70 ft before arrivals refracting from its top surface could be detected. The velocity contrasts between successive layers in Fig. 14 are high, and at first sight this example might seem to be an ideal case for refraction mapping. Reference 4 uses a wave-front analysis to show how this apparent anomaly occurs.

Soske indicates that the problem can be overcome by firing a shot in a deep hole such that arrivals from the intermediate layer are recorded at the surface. Of course, it would be necessary that the existence of the intermediate layer be known beforehand because of some other source of information, such as a drill hole, before this would normally be attempted. If a time-distance curve shows a very large velocity contrast between the first and second layers, the existence of a blind zone might be suspected. The error that results from not knowing the existence of a blind zone is that the computed-depth to the refracting layer is too shallow. However, even in the worst case, it is doubtful whether the error would approach 50%.

If the presence of a blind zone is suspected, the following procedure can be used to determine the maximum thickness of such a layer (Z_2) that could exist and still not be manifested by first arrivals on the time-distance curve.

Let us assume that a straightforward interpretation of a time-distance curve

results in some value for Z_1. This is the maximum value of Z_1, and it is obtained by ignoring the possibility that an intermediate layer exists. If there is a blind zone, however, there will be an infinite number of combinations of Z_1 and Z_2, with Z_2 ranging up to its maximum, undetectable thickness, at which value Z_1 will be a minimum. The combined thickness of the first two layers (Z_{12}) can lie anywhere between the limits:

$$Z_{12}(\text{min}) = Z_1(\text{max}) + 0,$$

and

$$Z_{12}(\text{max}) = Z_1(\text{min}) + Z_2(\text{max}),$$

where Z_2(max) is the maximum, undetectable thickness of the second layer and Z_1(max) is the value of Z_1 obtained from the time-distance curve. Based on the material in Refs. 5 and 6, the following statements can be made:

$$Z_2(\text{max}) = \frac{RS}{R+S} Z_1(\text{max}), \qquad (17)$$

$$Z_1(\text{min}) = Z_2(\text{max})/R, \qquad (18)$$

where:

$$R = \frac{Z_2}{Z_1},$$

and is obtained from the chart in Fig. 15, and

$$S = \frac{\tan \alpha_{23}}{\tan \alpha_{13}},$$

where: $\alpha 23 = \sin^{-1} V_2 / V_3$,

$$\alpha 13 = \sin^{-1} V_1 / V_3.$$

As an illustration of the procedure for determining Z_2(max), consider the following example: A time-distance plot shows two velocities, 2,300 and 14,000 ft/sec, and it is suspected that there is a hidden layer between the low-velocity (2,300 ft/ sec) surface layer and the 14,000-ft/sec refractor. A value for Z_1 of 37 ft is obtained from the time-distance curve. If we assume that a probable velocity for the suspected blind zone is 7,500 ft/sec, how thick could it be and still not be detected by first arrivals? From the available information and the assumed value of V_2, we can write:

Z_1(max) = 37 ft (determined from the time-distance curve by an intercept time)

$$\alpha_{12} = \sin^{-1} \frac{2,300}{7,500} = 17.9 \text{ deg}$$

$$\alpha_{23} = \sin^{-1} \frac{7,500}{14,000} = 32.5 \text{ deg}$$

$$\alpha_{13} = \sin^{-1} \frac{2,300}{14,000} = 9.5 \text{ deg.}$$

On Fig. 15, we determine the value of R by locating the intersection of α_{12} = 17.9 deg and α_{23} = 32.5 deg, and interpolating between the R-lines; R is seen to be approximately 0.62. To find the value of S:

$$S = \frac{\tan \alpha_{23}}{\tan \alpha_{13}} = \frac{\tan 32.5 \text{ deg}}{\tan 9.5 \text{ deg}}$$

$$= \frac{0.64}{0.167} = 3.8;$$

so that from Eq. (17):

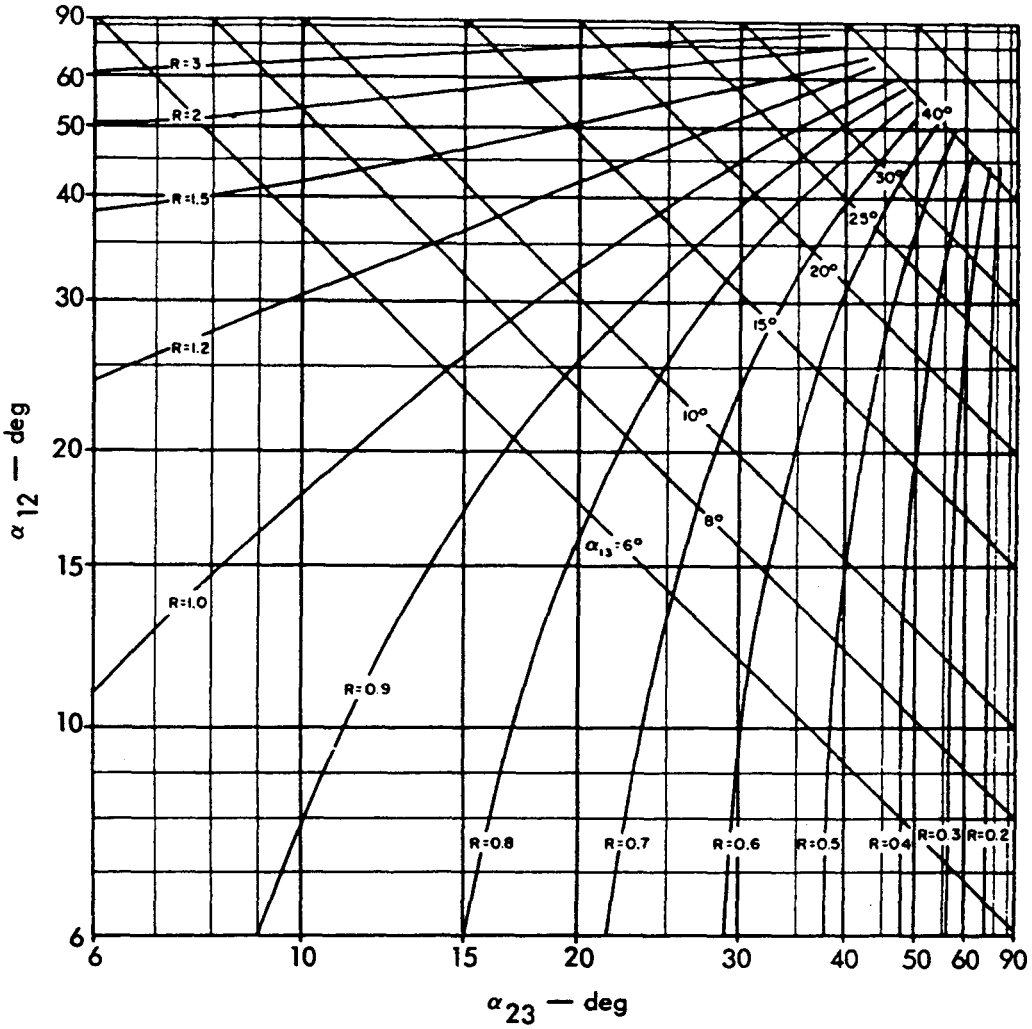

Fig. 15. Nomograph to be used in determining maximum thickness of possible hidden layer (taken from Fig. 90(b), p. 148, of Leet[5] - based on Maillet and Bazerque, "La Prospection seismique du sons-sol" Annales des Mines, XX, Douzieme Serie, p. 314, 1931).

$$Z_2(\text{max}) = \frac{0.62 \times 3.8}{0.62 + 3.8} 37$$

$$\simeq 20 \text{ ft},$$

and from Eq. (18):

$$Z_1(\text{min}) = \frac{20}{0.62}$$

$$\simeq 32 \text{ ft}.$$

Therefore, the maximum undetectable thickness of the hidden layer is 20 ft, and the combined thickness of the first two layers can range from a minimum of 37 ft (no intermediate layer) up to a maximum of 52 ft; i.e., Z_1(min) + Z_2(max).

The hidden layer problem can be a serious drawback to shallow surveys with the refraction seismograph. The possibility of such a layer's existence emphasizes the desirability of using an exploratory drill in conjunction with seismic surveys whenever possible.

Another functional problem than can occur in refraction surveys is the existence of a velocity reversal that will result in erroneous computations of depths

to underlying beds. A velocity reversal can exist because of a low-velocity layer or because of a high-speed layer. In either case velocities do not increase progressively with depth, and at some point in the stratigraphy there is downward transition to a relatively lower velocity. This has the effect of refracting the seismic ray downwards towards the vertical as shown in Fig. 16. Refractions from such a low-velocity layer cannot be detected at the surface, and the existence of this layer cannot be determined from the time-distance curve. In fact, the ray will not return to the surface until it encounters a layer with a velocity higher than any layer previously encountered in its downward travel.

In certain unusual circumstances in which the velocity of the bed immediately overlying the low-velocity layer increases. with depth, a "shadow zone" may result at the surface where no first arrivals at all

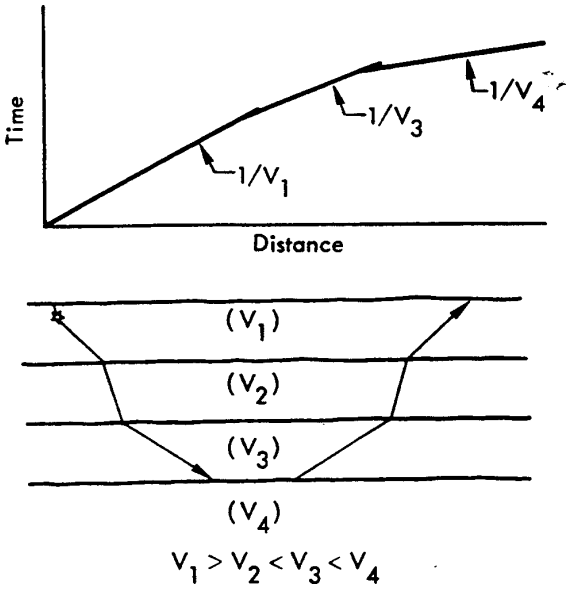

Fig. 16. Velocity reversal and corresponding time-distance curve.

are detected, and in similar circumstances the time-distance curve may show a sudden jump in time at a specific distance.[5,7]

The effect of a low-velocity layer is to make the computed depths larger than actual depths. If the presence and velocity of a low-velocity layer are known, the layer can be compensated for in the computations, but its existence must be determined by means of a more direct method, such as an uphole velocity survey. Fortunately, velocity reversals are seldom encountered in shallow surveys.

There is a third type of velocity-depth situation, a continuous increase of velocity with depth that rarely occurs but still warrants a brief discussion. This type of situation can exist because of a finely stratified geology or because of a progressive decrease of weathering with depth. A continuous increase of velocity with depth will manifest itself in a time-distance curve similar to the one shown in Fig. 17.

This type of curve can be transformed into a curve of velocity vs depth by means of the following equation[8]:

$$Z_S = \frac{1}{\pi}\int_0^S \cosh^{-1}\frac{V_S}{V_X}\,dX, \qquad (19)^*$$

where:

Z_S = depth at which velocity is V_S

V_S = velocity (from time-distance curve) corresponding to distance S from shot point.

*This is the "Herglotz-Weichert-Bateman" equation.

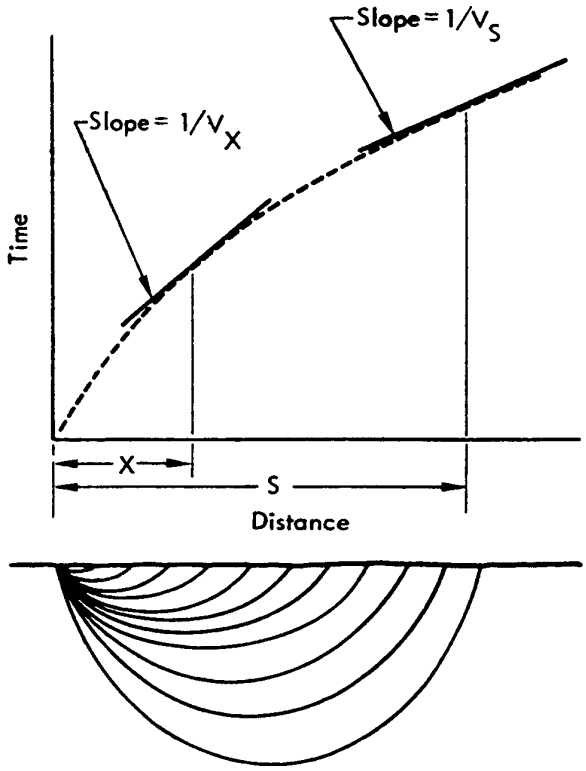

Fig. 17. Schematic of ray-paths and time-distance curve for continuous increase of velocity with depth.

V_X = velocity (from time-distance curve) corresponding to any distance X < S from shot point.

X = distance from shot point.

The integral is evaluated graphically by choosing a particular distance S and the corresponding velocity V_S, obtained from the tangent to the time-distance curve at S, and plotting values of $\cosh^{-1}(V_S/V_X)$ against X, where X is any distance less than S. The area under the resulting curve (obtained with a planimeter) is multiplied by $1/\pi$ to determine the depth, Z_S, at which the velocity is V_S. The integration is repeated for decreasing values of S, and the graph can then be constructed of the variation of velocity with depth. The method is tedious and should only be used when there is a smooth, continuous increase of velocity with depth. Often, gradual increases of velocity can be interpreted by assuming that the curved time-distance plot is made up of a few straight-line segments.

OTHER PROBLEMS AND LIMITATIONS

This section of the report outlines some of the drawbacks and difficulties that can affect seismic refraction investigations. The following discussion is not intended to leave the reader with an unfavorable impression of the refraction method, but merely to alert him to some possible problems that can influence the results of a survey. The refraction seismograph is a very powerful exploration tool, and its value will be enhanced by a realistic and knowledgeable operator. Reference 9 is an excellent summary of the problems of seismic investigations at shallow depths and will be of interest to engineers or geologists who routinely use refraction surveys; much of the following material is based on this reference.

Generally, as the depth of the investigation becomes shallower the limits of method are approached, and the problems inherent in the method increase. A large proportion of refraction surveys for engineering purposes are concerned with depths of the order of 50 to 75 ft and total times of 50 to 100 msec. It is apparent then that a millisecond is a large unit of time, and arrival times must be picked with an accuracy of a millisecond or less. This means that the charge weight, its surrounding medium and coupling, the

amplifier gains, and the placement of the geophones are all important factors in obtaining the sharp breaks required for accurate timing of first arrivals. An error of 1 msec corresponds to only 1 ft of depth with a first-layer velocity of 2,000 ft/sec, but the error would be 5 ft for a first-layer material with a velocity of 10,000 ft/sec.

it is necessary to maintain close control of overburden velocities and depths, particularly to distinguish travel time spent in the overburden from time spent in underlying, higher velocity layers. This is particularly so when there are more than two layers. Unconsolidated overburden deposits frequently show lateral changes in velocity over relatively short distances, and it is almost always desirable to fire at least one intermediate shot between the ends of the line.

Generally, when one is working with short lines, say 500 ft or less, obtaining sharp breaks will not be a problem, unless there is difficulty in burying sufficient explosive deep enough. Because of the attenuation of the explosive impulse . with increasing distance, and particularly because of the relatively greater attenuation of the high-frequency components, the arrivals tend to become less distinct and more rounded with increasing distance from the shot. The objective is to nick arrival times to within 1 msec or less, and to pick what appears to be the onset of the pulse. The presence of background noise, such as that generated by vehicle traffic, or weak arrivals caused by poor charge coupling, can make accurate determinations difficult.

Irregularities in a shallow bedrock surface have a more pronounced effect on accuracy than irregularities in a deeper horizon. A highly irregular refractor surface will tend to make delay-time methods somewhat inaccurate because the times being compared represent different depths, depending on the direction of the shot. This situation is depicted in Fig. 18. The effect of using delay times to compute depths will be to "smooth" a highly irregular surface. The situation is aggravated if the velocity contrasts are not large; i.e., if the horizontal offsets between the geophone and the point at which the ray emerges from the refractor ($\cong Z \tan \alpha$) are large.

Further complications arise if the rock surface is not only eroded and irregular, but also weathered. In this case the rock surface will not be a well-defined boundary but rather a zone of transition. In the case of layered rock, some of the layers may be better media for the transmission of seismic energy and the refractions may not necessarily be from the top of the rock. Also, as distance from the shot increases the higher frequency (i.e., shorter wavelength) energy is progressively absorbed and because of the signal's increasing wavelength, the energy

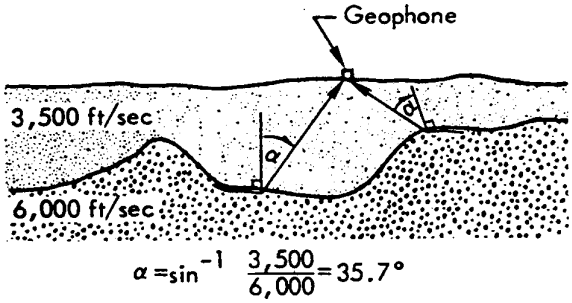

Fig. 18. Schematic of shallow, irregular refractor surface producing different first-layer travel times at same geophone from shots on either side of it.

may refract from progressively thicker beds. It is necessary to bear in mind that the wavelength becomes a significant factor when the refractor is of a limited thickness. Long wavelength seismic signals do not "see" thin beds.

Some materials may be anisotropic, i. e., there may be differences between horizontal and vertical velocities, or even between horizontal velocities in different directions. These differences may be as large as 40% in some materials. Rocks with finely bedded structure, such as sandstones and shales, generally exhibit some degree of anisotropy.

There is no hard and fast guidance for a sequence of steps to be followed when interpreting or reducing travel-time curves. Straightforward two- or three-layer plots with well-defined straight-line segments representing each layer will probably be the exception rather than the rule. Overburden velocities may change along the length of the line, there may be relief in the refracting horizons, layers may pinch out, and breakover points (i.e., critical distances) in the plots may not be readily apparent.

The first step is to attempt to identify the layers present according to their velocities, and then to determine which arrival times correspond to the various layers. Where the arrivals do not line up in straight lines, identification can be attempted by plotting differences in overlapping arrival times for those believed to be from the same refractor. Also, delay times can be computed and plotted below the arrival times, and the lineups, or lack thereof, of the reduced times will assist in assigning velocities to the various layers and sorting the arrival times. In the same context that there does not exist a standard sequence of interpretational steps, the interpreter should not feel constrained by a rigid format, but should rather attempt a number of methods according to his judgment. Some knowledge of geology is helpful in reconciling the interpretation with what is reasonable from a structural geology standpoint.

Some refraction data obtained in complex geology will be very puzzling to the interpreter. There is always a reason why the arrival times are as they are, although it is not always apparent. Some cases are simply not amenable to straightforward interpretation using the methods already described. There are other techniques, generally involving the construction of wavefront diagrams,[10,11] that are available for analyzing complex cases; however, they are time-consuming and tedious to apply, and are beyond the scope of this report.

Domalski[9] states: “The basic difficulty in the interpretation of a shallow refraction survey consists not so much on the choice of a suitable method, on which to base the interpretation, as on the correct decision regarding the various aspects of the results. In other words, the information which is normally obtained from the examination of the time-distance curves cannot be accepted entirely at its face value.” He concludes his paper on a more positive note by saying: “Results obtained from shallow investigations are useful because they provide rapidly a picture of the bedrock configuration, and guide a subsequent drilling programme.”

As stated at the beginning of this section, this discussion of potential problems was intended to alert the reader to possible difficulties and not to discourage the application of the technique. In fact, it is believed that the method is not used widely enough in exploration programs. When the refraction seismograph is used wisely, and particularly when allied with the exploratory drill, it will invariably speed the recovery of subsurface information and reduce site investigation costs.

ADDITIONAL TECHNIQUES

The refraction seismograph is fundamentally an accurate timing device and can be applied to exploration situations other than routine refraction surveys along the ground. The method can be modified for use over water, and the equipment can be used for measuring velocities in drill holes. This section will discuss some of these techniques.

The first problem for consideration is that of running a refraction survey across a river. Normal procedure would require that a line of detectors be laid across the bottom of the river or ,floated on the water surface. Both these procedures require special cables and detectors and they are, therefore, often impractical. However, because shot and detector are theoretically interchangeable in refraction work, the normal arrangement of having detectors along a line across the river with shots on the banks can be reversed so that the detectors are on the banks and the shots are in the river. This arrangement is illustrated in Fig. 19.

A series of small charges are detonated on the river bottom along a line across the river. It is required that the detector on the far bank from the seismograph be connected to the recording instrument by means of a cable running across the river. It is required, further, that the distance of the shot from the

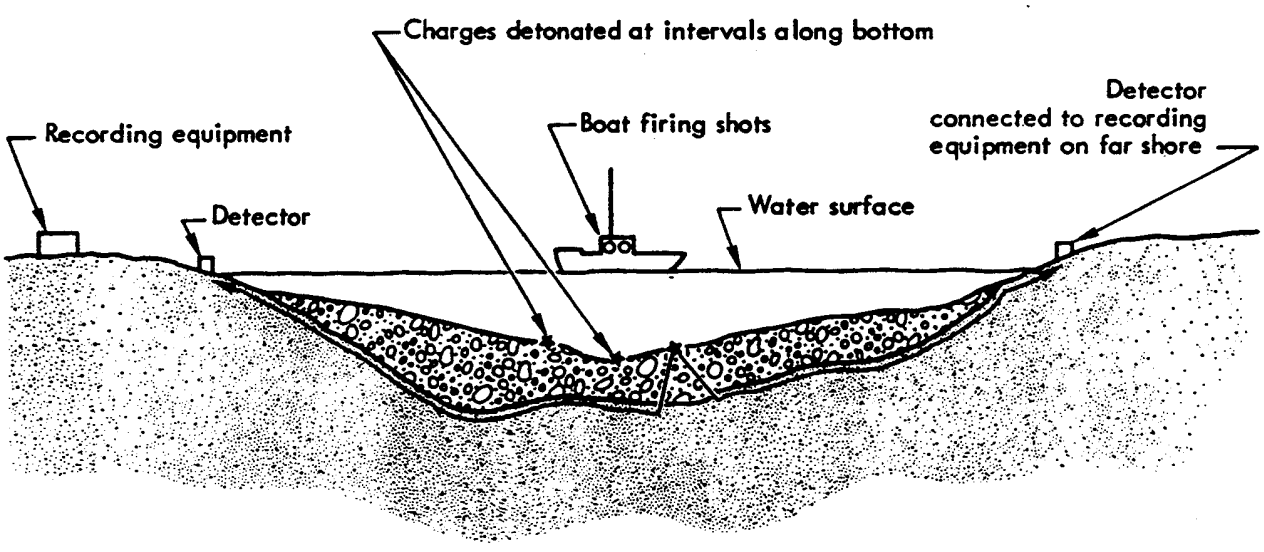

Fig. 19. Schematic of refraction survey across body of water.

detectors be surveyed and known, and that the shot instant be transmitted to the seismograph. The latter can be done either by hard wire or, if the equipment is available, by radio transmission. The usual practice is to fire the shots from a small boat and to locate its position by transit triangulation. It is not necessary that the shots be fired at even increments of distance across the river. In some cases the distance from shot to detector has been determined by recording the direct arrival of the explosive impulse through the water. If the detectors are placed very close to the water's edge, the shock arrival through the water can often be seen on the record as a high-frequency signal. With the water velocity known (4,800 ft/sec±), the distance to the shot is easily determined. The arrival times and distances are plotted and interpreted in the normal fashion. This method is an expedient technique for dam site exploration when knowledge of the thickness of river bottom deposits is needed.

In some cases of overwater surveys it may not be possible to place detectors on the ground simply because the body of water is too large, as in the case of a bay or a lake. In these cases it will be necessary to employ either a floating or submerged cable with hydrophones instead of geophones. The floating cable has the advantage that it can be towed along the line of exploration. Either way two boats will be required, one containing the recording instruments and towing cable and the other being used as a shot-firing boat. A radio-transmitted time break is a necessity for this type of work.

It is possible for loose, unconsolidated bottom sediments in bays and estuaries to have a lower velocity than that of sound in water. 12 and in such a case the direct arrival through the water will obscure the arrival of energy through the sediments. A special low-pass filter to block the high-frequency arrival through the water is then required.

The refraction seismograph can be used to measure vertical velocities in boreholes. Such uphole surveys are a valuable adjunct to conventional refraction exploration because they provide a vertical velocity profile and will indicate the presence of a low-velocity layer, if one exists. The term uphole refers to placing shots in a drill hole and recording arrival times at the surface. The reverse of this procedure is called a downhole survey, and is conducted by firing shots at the surface and recording arrivals down the hole, usually by means of a multidetector cable. Downhole surveys require that the hole be filled with fluid, or that a geophone capable of being coupled to the wall of the hole be available. The principles are the same in both cases, but an uphole survey, which has the advantage of requiring no special equipment, usually destroys the borehole.

In practice, a string of small explosive charges is preassembled so that the charges are spaced at the desired intervals. Each charge has a separate firing line and the entire assembly is suspended in the hole and fully stemmed to prevent the explosives being blown out of the hole. The interval between charges will depend on the depth of the hole and the amount of detail desired. Charge spacings of 5 to 10 ft are typical for holes 50 to 100 ft deep, and it is evident that the charges must be detonated one by one in a sequence

starting at the bottom - otherwise the firing lines will be cut. Charge weights of the order of 1 /4 lb. or less are typical. Several geophones are placed near the hole collar, say 5 to 10 ft from it, and the average arrival time is used. The arrangement for. an uphole survey is shown in Fig. 20 together with the plot of arrival times measured at the surface. The slant distance from shot to geophones must be used for the shots near the top of the hole.

It will be noted that the velocities derived from the arrival times in Fig. 20 do not always correspond exactly to the nominal velocities of the various layers. The differences between the actual velocities and those based on the arrival times shown in Fig. 20 are representative of the precision to be expected in the typical

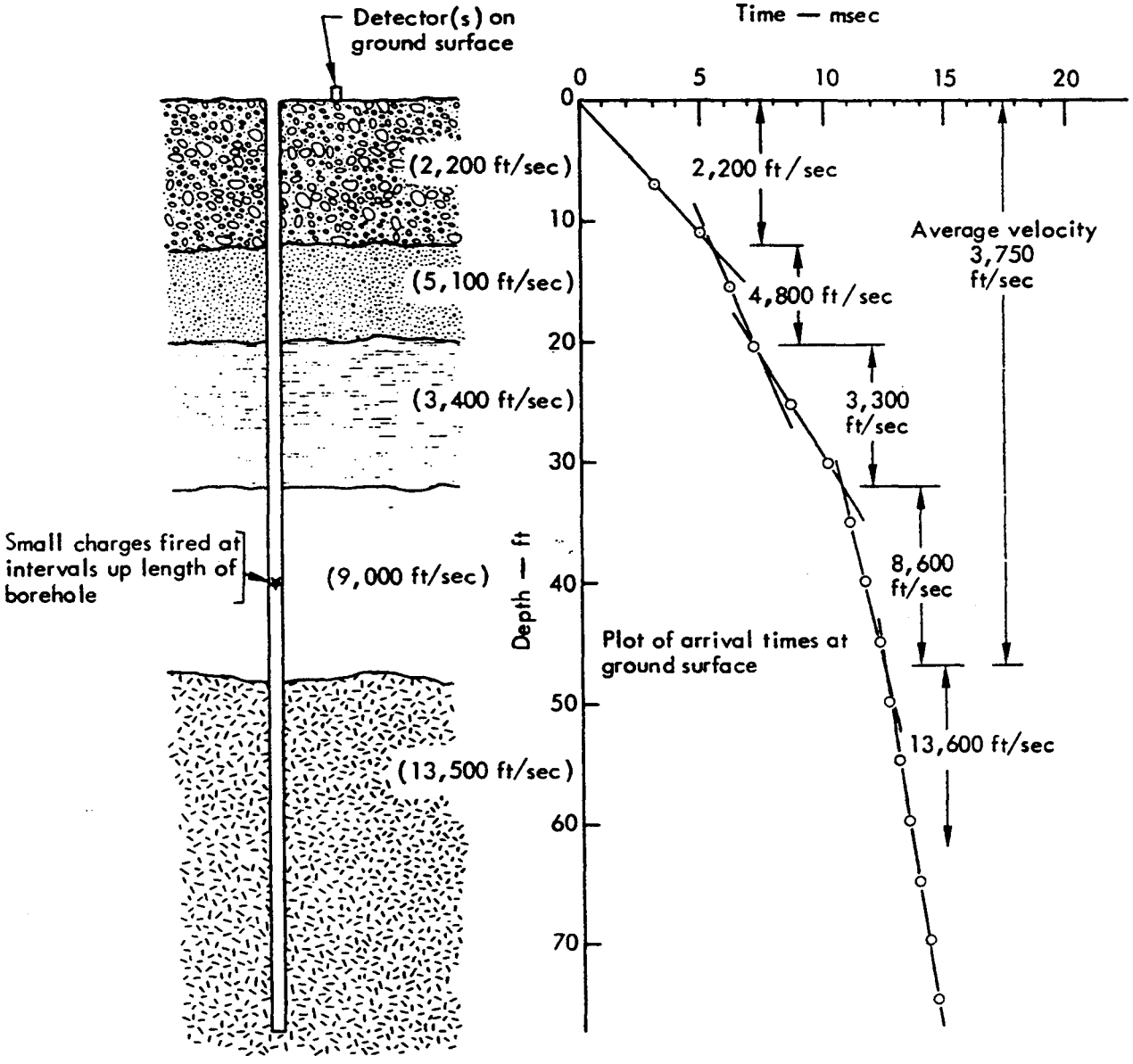

Fig. 20. Example of uphole survey and corresponding plot of arrival times.

borehole survey. Further, it is not uncommon for a discrepancy to exist between the velocities obtained from a borehole velocity survey and those observed in refraction surveys. There are several reasons for such a discrepancy. As previously indicated, some materials show anisotropy in their seismic velocities, particularly finely bedded sediments. Also, a low-velocity layer will not be apparent on a refraction time-distance curve, but it will be detected in a borehole survey. If a discrepancy does exist, it is not generally large and, unless it is due to a low-velocity layer, there is usually no need to correct refraction surveys on the basis of the borehole velocity data.

An interesting variation of the uphole survey is developed by Meissner13 in which a conventional seismic line is laid out radially away from the hole collar so that arrival times from each uphole shot are recorded along the entire seismic cable. Wave fronts of the seismic energy are constructed by connecting points of equal travel times. The assumption is

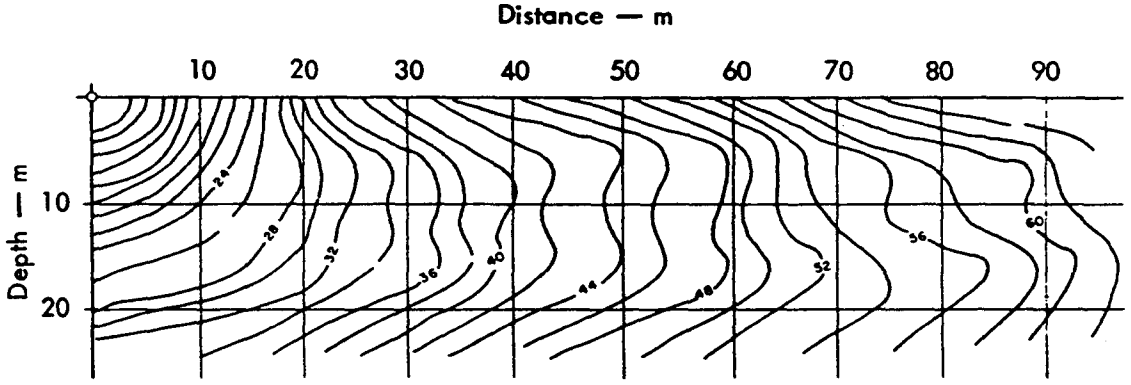

Fig. 21a. Meissner wave-front diagram showing high-velocity layer at depth of 5 to 16 m (taken from Fig. 5, p. 536, of Meissner[13] —used with permission).

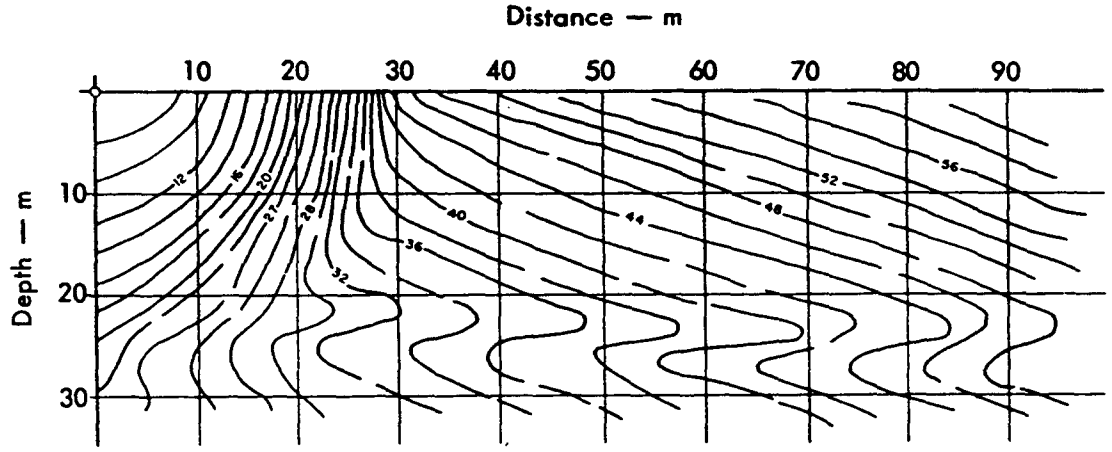

Fig. 21b. Meissner wave-front diagram showing thin high and low-velocity layers (taken from Fig. 6, p. 537, of Meissner[13] - used with permission).

made that the travel time from a shot at depth Z to a geophone on the surface at a distance X from the hole is the same as that from a (fictitious) shot at the top of the hole to a (fictitious) geophone at a distance X and a depth Z. Unless the beds are reasonably flat lying and the terrain is level, this assumption will lead to errors.

A separate travel-time curve is generated by each uphole shot. The wave fronts are constructed by plotting the arrival times at each geophone at a depth beneath that geophone location equal to the depth of the shot in the hole. Points of equal travel times are then contoured to give a wave-front diagram. Two examples of the results of this technique are shown in Fig. 21. The method provides a qualitative picture of subsurface conditions as an adjunct to the standard uphole information. Meissner presents examples of wave-front diagrams for other geological conditions in his paper.[13]

The main sources of error in this technique are small, local inhomogeneities within the near-surface layer and the presence of dipping high-velocity layers. Also, an elevation change along the seismic line imposes a delay or an advance on all wave-front times below the line; therefore, this type of survey should be carried out on flat ground if possible.

Field Procedures

This section recommends general field procedures for conducting refraction surveys. The first consideration in a refraction survey is the interval between the geophones. The spacing will depend on the depth of exploration and the subsurface detail desired. As a rule of thumb, the total spread length should be three to five times the maximum depth anticipated. Changes in geophone spacing can be made in response to the data observed in the field; i.e., by picking and plotting records as they are obtained. The total spread length will obviously determine the geophone interval to some extent; however, there is no requirement to have a constant spacing over the length of the line. It is sometimes desirable to shorten the spacing between geophones at each end of the line, at least for the first few lines run in a new area. This practice will provide more complete data on overburden velocities.

Seismic cables are manufactured with fixed spacings; i.e., the "take-out" or polarized connector for each detector is molded into the cable. It is desirable to have several cables available with different spacings, such as 25, 50, and 100 ft. The 25-ft spacing is most applicable to the bulk of engineering surveys, which are seldom directed towards explorations deeper than 50 or 100 ft.

The cable is laid out along the ground in a straight line. If the terrain along the line has any relief, surveys will be required so that layer thicknesses can later be plotted in true elevation.

The shots at the ends of the cable should be offset at a right angle to the cable and not beyond the end in line with the cable. This arrangement is illustrated

in Fig. 22. The purpose of the right-angled offset is to allow determination of the total times; i.e., the travel time from each shot to the far geophone. The travel time from a shot beyond the end of the cable, in line with it, will be greater than the total time. The offset distance, usually 5 to 15 ft, normally provides a direct arrival through the surface layer and allows a determination of its velocity. The slant distances from shot to geophone must be computed for plotting arrival times at the first two or three geophones.

As discussed in the section on interpretation, it is always advisable to fire supplementary shots along the length of the line in order to provide as much information as possible about the depth of the overburden and possible variations of its velocity. The necessity for these shots can be determined as the survey program progresses; however, it should be standard procedure to fire at least one shot at the center of the seismic cable, even for short lines with a 25-ft spacing.

There is no fixed rule for the distance a beyond-the-end shot should be from the end of the cable. In most cases the distance need not even be measured because we are usually interested only in the relative times obtained from such a shot. The objective of a beyond-the-end shot is to record refracted arrivals from the layer we are trying to map, and to record those refractions at as many geophones as possible. A distance somewhere between half the cable length and the whole cable length is usually adequate. If a number of refraction lines are to be surveyed end to end, it is advisable to locate the beyond-the-end shots at exactly half the cable length or a whole cable length from the end; i.e., so that they will coincide with the middle or end shot of the adjacent geophone array.

The data points should be plotted on a convenient scale; it is generally best if the time and distance scales are approximately the same length. It is helpful if different symbols are used to designate arrival times for each shot; this particularly helps to avoid confusion where the time-distance curves cross each other. It is suggested that faint, dashed lines be used to connect all the arrival times for each shot. The straight line portions of the plots, if any, can be joined by heavier lines, projected back for time intercepts, and labeled with their corresponding velocities.

Charge weights adequate to produce sharp first arrivals will vary with geology, length of line, and amount of background noise. Weights may vary from only a blasting cap for a 100-ft line to

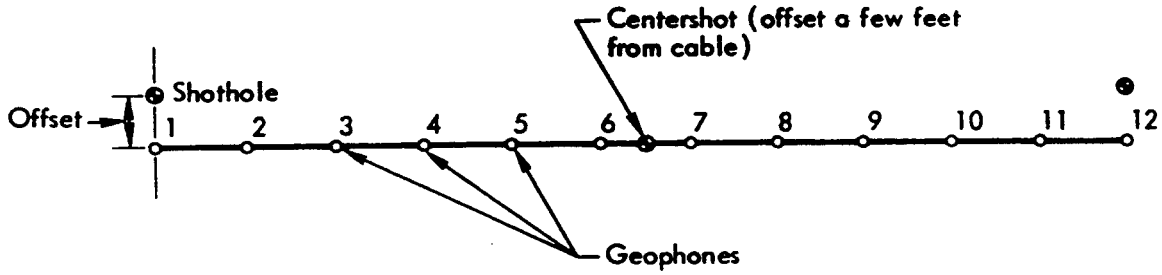

Fig. 22. Recommended shot layout pattern for seismic line.

several pounds for long lines under adverse conditions. Generally a few ounces in a shallow 1- or 2-ft hole will be adequate for a 275-ft line. Coupling of explosive energy can be improved by burying charges deeper and saturating the shot hole with water. An emplacement hole can often be formed with a heavy steel bar driven into the ground. Figure 23 shows a seismograph record from a 275-ft line in which adequate first arrivals have been obtained at each geophone. Note the rounding of the breaks with increasing distance from the shot.

Special blasting caps are made for seismic work; e.g., Dupont SSS Seismograph or Atlas Staticmaster. The use of if instantaneous" standard caps should be avoided because they can have a delay of up to 15 msec between application of current and detonation, and further, this delay is not constant. Almost all seismographs indicate zero-time when the current is applied to the cap. The special seismograph caps will detonate in less than 1 msec after application of current.

The geophones must be firmly coupled to the ground. There are a variety of geophone bases, such as a spike or a tripod, to suit the type of ground surface. The spike-type of base is probably the most common; the spike is pushed into the soil to provide a rigid coupling with the ground surface.

A 12-channel seismograph that produces a visual record of the waveforms arriving at each geophone is preferred over the single-channel seismographs that are available for shallow investigations. These small, single-channel

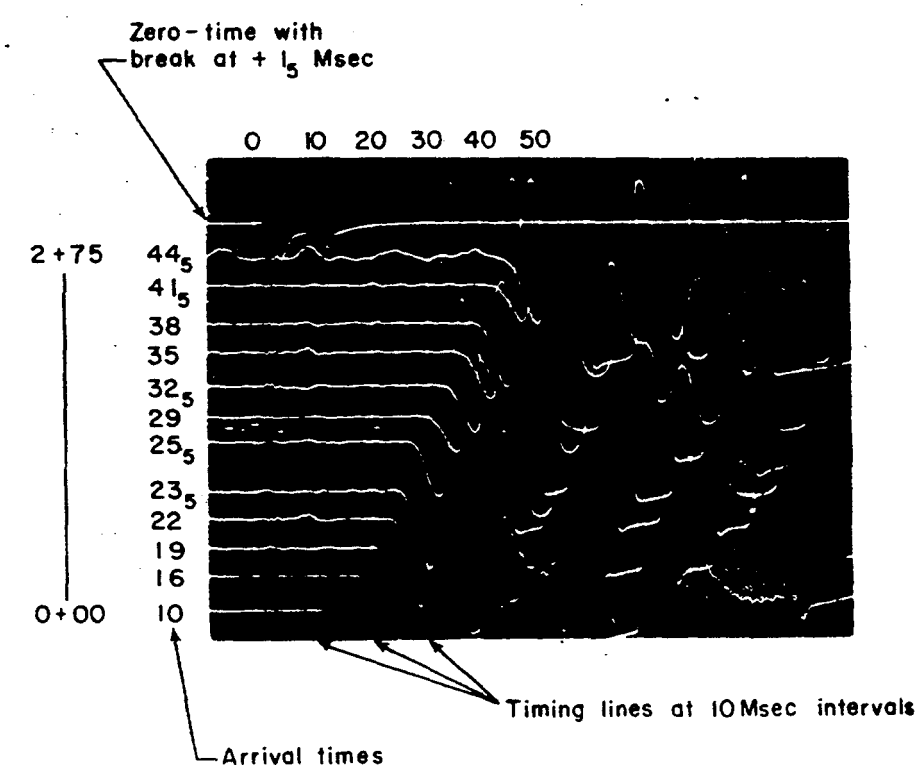

Fig. 23. Example of seismic record on Polaroid film obtained with portable engineering seismograph.

instruments indicate arrival times by different methods, such as neon lamps, glow tubes, dashes on paper, or oscilloscope displays. Although light and compact, they are suited only for very shallow work and suffer from the disadvantage of not simultaneously displaying the complete set of arrivals at all geophones. There is often some judgment required in picking first arrivals from a seismograph record, particularly if noise is present, and a machine that records the complete set of waveforms allows the exercising of this judgment.

There are several 12-channel instruments commercially available, generally as a complete package including cable and geophones. They all employ light-beam galvanometers and record the signals either on Polaroid film or on a continuous roll of photo-sensitive paper. These instruments are well-suited for engineering use.

A valuable accessory in the conduct of refraction surveys is a blasting machine that can transmit the zero-time to the recorder by means of radio. This capa-bility allows much greater flexibility in field operations and means that beyond-the-end shots can be made without the need to manipulate large quantities of wire. Such a device is particularly desirable for overwater surveys. It is a fairly straightforward task to build such a blasting machine and to use ordinary Citizens Band radios to transmit and to receive the zero-time. One approach is to transmit a tone and have the detonation of the cap interrupt the tone.

Conclusions

This report has covered the fundamentals of seismic refraction theory and interpretation. It is recognized that it may be difficult to arrive at an understanding of refraction surveying only by reading about it. However, it is hoped that this document, when combined with actual field experience, will assist the reader in acquiring a working familiarity with the technique. For those who have been using the refraction seismograph, and who may have learned something new from this report, it is suggested that they consider reevaluating some of their previous surveys.

The methods of interpretation described in this report are not the only methods available, but it is believed that they are the most applicable ones for the majority of engineering surveys, and they are also the simplest. In those cases where the strata are reasonably flat lying, depths computed by time-intercepts will generally be adequate. Wherever the time-distance plots reveal, by their undulations or irregularities, the existence of something more complex, the delay-time method should be attempted.

Recommendations have been made about the desirability of using refraction surveys in conjunction with a drilling program. This point cannot be overemphasized. Exploratory drilling is almost always done in a site investigation; its value, in terms of the quality of information gathered, will be enhanced if refraction surveys are carried out first and the

results used to guide the drilling operations. Even if some of the refraction data appears complex, ambiguous, or just plain peculiar, this in itself is information, and those refraction surveys will have designated areas in which drilling will provide more useful information. Conversely, stratigraphy obtained from a drill hole is very often helpful in interpreting a refraction profile. Because the velocity of geologic material is in itself a useful index, borehole surveys (e.g.. uphole) warrant serious consideration as a follow-up investigation for selected areas, particularly if a hidden layer is suspected.

The refraction seismograph offers a rapid, inexpensive, and accurate method of subsurface exploration. Its application to site investigations should be the routine rather than the exception.

References

1. M. B. Dobrin, Introduction to Geophysical Prospecting (McGraw-Hill, New York, 1960).

2. J. J. Jakosky, Exploration Geophysics (Trija Publishing Co., Newport Beach, Calif., 1957).

3. L. V. Hawkins, “The Reciprocal Method of Routine Shallow Seismic Refraction Investigations,” Geophysics 26, 806-819 (1961).

4. J. L. Soske, “The Blind Zone Problem in Engineering Geophysics”, Geophysics 24, 359-365 (1959).

5. D. L. Leet, Practical Seismology and Seismic Prospecting (D. Appleton-Century Co., New York, 1938).

6. R. Green, “The Hidden Layer Problem”. Geophys. Prospect. 10, 166-177 (1962).

7. L. B. Slichter, “The Theory of the Interpretation of Seismic Travel-Time Curves in Horizontal Structures,” Phys. 3, 273-295 (1932).

8. B. B. Redpath, “Seismic Investigations of Glaciers on Axel Heiberg Island;” in Axel Heiberg Island Research Reports, Geophysics No. 1, McGill University, Montreal, Quebec, 1965.

9. W. Domalski, “Some Problems of Shallow Refraction Investigations;” Geophys. Prospect. 4, 140-166 (1956).

10. H. R. Thornburgh, “Wave-front Diagrams in Seismic Interpretation;” Bull. Am. Assoc: Petroleum Geologists 14, No. 2 (1930).

11. J. G. Hagedoorn, “The Plus-Minus Method of Interpreting Seismic Refraction Sections,” Geophys. Prospect. 7, 158-182 (1959).

12. C. B. Officer, “A Deep-Sea Seismic Reflection Profile;” Geophysics 20, 270-282 (1955).

13. R. Meissner, “Wave-front Diagrams from Uphole Shooting,” Geophys. Prospect. _9, 533-543 (1961).

14. Subsurface Investigation-Geophysical Explorations, U. S. Army Corps of Engineers, Washington, D. C., Engineering Manual EM-1110-2-1802 (1948).

Bibliography

Black, R. A., F . C. Frisehknecht, R. M. Hazlewood, and W. H. Jackson, Geophysical Methods of Exploring for Buried Channels in the Monument Valley Area, Arizona and Utah, U. S. Geological Survey, Bulletin 1083-F, 1962.

Burke, K. B. S., "A Review of Some Problems of Seismic Prospecting for Groundwater in Surficial Deposits," in Mining and Groundwater Geophysics, 1967, Geological Survey of Canada, Economic Report No. 26, Ottawa. Canada, 1970.

Bush, B. O., and S. D. Schwarz, Seismic Refraction and Electrical Resistivity Measurements over Frozen Ground, National Research Council of Canada. Associate Committee on Soil and Snow Mechanics, Technical Memorandum No. 86, Ottawa, Ontario, 1965.

Grant, F. S., and G. F. West, Interpretation Theory in Applied Geophysics (McGraw-Hill, New York, 1965).

Griffiths, D.H., and R. F. King, Applied Geophysics for Engineers and Geologists (Pergammon Press, Inc., New York, 1965).

Hales, F. W.; “An Accurate Graphical Method for Interpreting Seismic Refraction Lines,” Geophys. Prospect. 6, 285-294, 1958.

Hawkins, L. V., and D. Maggs, "Nomograms for Determining Maximum Errors and Limiting Conditions in Seismic Refraction Surveys with a Blind Zone Problem, Geophys. Prospect. 6, 526-532, 1961.

Heiland, C: A., Geophysical Exploration Hafner Publishing Co.. New York, 1963).

Hobson, G. D., "Seismic Methods in Mining and Groundwater Exploration," in Mining and Groundwater Geophysics, 1967, Geological Survey of Canada, Economic Report No. 26, Ottawa, Canada, 1970.

Linehan, D., and V. J. Murphy, "Engineering Seismology Applications in Metropolitan Areas," Geophysics 27, 213-220, 1962.

Musgrave, A. W., Ed., Seismic Refraction Prospecting, Society of Exploration Geophysicists, Tulsa, Okla., 1967.

Schwarz, S. D., Site Evaluation-Geophysical Exploration, Fifth Chicago Soil Mechanics Lecture Series, 1970.

Scott, J. H., B. L. Tibbetts, and R. G. Burdick. Computer Analysis of Seismic Refraction Data, U. S. Dept. of Interior, Bureau of Mines, Washington, D. C., RI 7595, 197 2.

Slotnick, M. M., Lessons in Seismic Computing, Society of Exploration Geophysicists, Tulsa, Oklahoma, 1959.

Tarrant, L. H., "A Rapid Method of Determining the Form of a Seismic Refractor from Line Profile Results," Geophys. Prospect. 4, 131-139, 1956.

Wyrobeck, S. M„ "Application of Delay and Intercept-Times in the Interpretation of Multilayer Refraction Time Distance Curves;' Geophys. Prospect. 4, 112-130, 1956.

Zirbel, N. N., “Comparison of Break-Point and Time-Intercept Methods in Refraction

,

Appendix A

Material Velocities

Tables A1, A2, and A3, which list the longitudinal wave velocities of various materials, have been selected from a number of publications[1,2,14] They are presented here as a series of separate tables, and no attempt has been made to construct a "universal" table of velocities. The tables are included to give some idea of what velocities mean in terms of geologic media.

Table A1. Speed of propagation of seismic waves in subsurface materials.[14]

MATERIALS	FEET PER SECOND
TOP SOILS:	
LIGHT AND DRY	600 TO 900
MOIST, LOAMY OR SILTY	1,000 TO 1,300
CLAYEY	1,300 TO 2,000
RED CLAY IN COLORADO (A)	1,630
SEMI-CONSOLIDATED SANDY CLAY (B)	1,250 TO 2,150
WET LOAM (B)	2,500
CLAY, DENSE AND WET - DEPENDING ON DEPTH	3,000 TO 5,900
RUBBLE, OR GRAVEL (B)	1,970 TO 2,600
CEMENTED SAND (B)	2,800 TO 3,200
SAND CLAY (B)	3,200 TO 3,800
CEMENTED SAND CLAY (B)	3,800 TO 4,200
WATER SATURATED SAND (B)	4,600
SAND (B)	4,600 TO 8,400
CLAY, CLAYEY SANDSTONE (B)	5,900
GLACIAL TILL UPPER SUSQUEHANNA (C)	5,600 TO 7,400
GLACIAL MORAINE DEPOSIT, DRY-CALIFORNIA (A)	2,500 TO 5,000
GLACIAL MORAINE DEPOSIT, SATURATED-CALIFORNIA	5,000 TO 7,000
CEMENTED LAVA AGGLOMERATE, CALIFORNIA (A)	5,000 TO 6,000
LOOSE ROCK-TALUS	1,250 TO 2,500
WEATHERED AND FRACTURED ROCK	1,500 TO 10,000
SHALE:	
OLENTANGY RIVER, OHIO	9,000 TO 11,000
UPPER SUSQUEHANNA (C)	10,200 TO 12,800
PANAMA CANAL ZONE	7,000 TO 8,000
MANCOS, COLORADO (A)	2,600 TO 2,900
ROMNEY SHALE-SHENNANDOAH RIVER - WEATHERED	4,000 TO 6,500
ROMNEY SHALE-SHENNANDOAH RIVER - GOOD	12,000
JOHN MARSHALL DAM SITE	2,900 TO 4,250
PHYLITE-YORK, PA. (D)	10,000 TO 11,000
SANDSTONE: (B)	7,200 TO 7,900
DEVONIAN-UPPER SUSQUEHANNA (C)	14,000
CANAL ZONE, PACIFIC END	7,000 TO 9,000
COLORADO, DENSE, HARD, AND CONTINUOUS WITH FEW SEAMS (A)	7,250
COLORADO, CONTAINING WEATHERED SEAMS AND SOFT AREAS. (A)	4,725
SMOKY HILL RIVER, KANSAS	6,000 TO 7,500
SANDSTONE CONGLOMERATE (B)	8,000
CHALK:	
FORT RANDALL DAMSITE - ABOVE WATER TABLE	6,300 TO 7,000
FORT RANDALL DAMSITE - BELOW WATER TABLE	8,000

MATERIALS	FEET PER SECOND
GRANITE:	
SIERRA NEVADA RANGE, CALIFORNIA (IN ROAD CUTS)	
FRIABLE AND HIGHLY DECOMPOSED	1,540
BADLY FRACTURED AND PARTLY DECOMPOSED	2,200
SOFTENED AND PARTLY DECOMPOSED BUT SLIGHTLY SEAMED	10,530
SOLID AND MONOLITHIC 70 FEET DEEP	18,500
NEW HAMPSHIRE (C) (COMPARISON OF VELOCITIES WITH DRILLING LOGS)	
BADLY BROKEN AND WEATHERED; FREQUENTLY ONLY CHIPS AND FRAGMENTS RECOVERED. SEGMENTS OF CORE LONGER, BUT WEATHERING HAD PENETRATED ABOUT 1/4 INCH ON EACH SIDE OF THE JOINT PLANES ON WHICH A FILM OF RESIDUAL CLAY HAD FORMED	3,000 TO 8,000
JOINT PLANES SHOW BUT LITTLE SIGN OF WEATHERING, EVEN THOUGH THEY ARE OPEN	10,000 TO 13,000
ENTIRELY UNWEATHERED AND UNSEAMED	16,000 TO 20,000
GRANODIORITE (B)	15,000
BASALT-CANAL ZONE-WEATHERED AND FRACTURED	9,000 TO 14,000
LIMESTONE, DOLOMITE, METAMORPHIC ROCKS, MASSIVE ROCKS (B)	16,400 TO 20,200
DIABASE, IN BED OF BROAD RIVER, SOUTH CAROLINA	19,700
GREENSTONE, TIGHT SEAMED-CALIFORNIA (A)	16,100
GREENSTONE, SLIGHTLY SEAMED-CALIFORNIA	13,300

NOTE:

(A) *Reported by G. A. Williams, U. S. Bureau of Public Roads*

(B) *From Report of Imperial Geophysical Experimental Survey in Australia*

(C) *Reported by A. E. Wood, Corps of Engineers*

(D) *Reported by L. T. Abele, Corps of Engineers*

Table A2. Approximate range of velocities of longitudinal waves for representative materials found in the earth's crust.[a]

A. *Classification According to Material*

Material	*Velocity**	
	Ft./Sec.	*M./Sec.*
Weathered surface material	1,000— 2,000	305— 610
Gravel, rubble, or sand (dry)	1,500— 3,000	468— 915
Sand (wet)	2,000— 6,000	610— 1,830
Clay	3,000— 9,000	915— 2,750
Water (depending on temperature and salt content)	4,700— 5,500	1,430— 1,680
Sea water	4,800— 5,000	1,460— 1,530
Sandstone	6,000—13,000	1,830— 3,970
Shale	9,000—14,000	2,750— 4,270
Chalk	6,000—13,000	1,830— 3,970
Limestone	7,000—20,000	2,140— 6,100
Salt	14,000—17,000	4,270— 5,190
Granite	15,000—19,000	4,580— 5,800
Metamorphic rocks	10,000—23,000	3,050— 7,020
Ice	12,050	

B. *Classification According to Geologic Age*

Age	*Type of Rock*	*Velocity*	
		Ft./Sec.	*M./Sec.*
Quaternary	Sediments (various degrees of consolidation)	1,000— 7,500	305— 2,290
Tertiary	Consolidated Sediments	5,000—14,000	1,530— 4,270
Mesozoic	Consolidated Sediments	6,000—19,500	1,830— 5,950
Paleozoic	Consolidated Sediments	6,500—19,500	1,980— 5,950
Archeozoic	Various	12,500—23,000	3,810— 7,020

C. *Classification According to Depth*†

	0—2000 ft. (0—600 M.) Ft./Sec.	2000—3000 ft. (600—900 M.) Ft./Sec.	3000—4000 ft (900—1200 M.) Ft./Sec.
Devonian	13,300	13,400	13,500
Pennsylvanian	9,500	11,200	11,700
Permian	8,500	10,000	.....
Cretaceous	7,400	9,300	10,700
Eocene	7,100	9,000	10,100
Pleistocene-to-Oligocene	6,500	7,200	8,100

* The higher values in a given range are usually obtained at depth.

† Data from B. B. Weatherby and L. Y. Faust, *Bull. Amer. Assoc. Petrol. Geologists*, 19 (1935) 1.

[a]Reprinted from pg. 660 of Jakosky[2].

Table A3. Velocities of seismic waves in rocks. [*a]

Material	Depth, ft	Longitudinal wave velocity, V_L, ft/sec
Granite	0	13,100–18,700
Norite, Sudbury	0	20,400
Basalt, Germany	0	18,300
Gabbro, Mellen	L40,000†	22,900
Diabase, Vinal Haven	L40,000	22,800
Dunite, Balsam Gap	L40,000	26,400
Cap rock (anhydrite, gypsum)	0	11,500–18,100
Dolomite	0	16,200–20,200
Dolomitic limestone	0	19,600
Salt, carnallite, sylvite	0	14,400–21,400
Alluvium	0	1,640– 6,600
Alluvium	6,500	9,800–11,500
Clay	0	3,300– 9,200
Limestone		
Arbuckle (Cambro-Ordovician)	0	17,400
Viola (Ordovician)	0	16,700
Viola (Ordovician)	4,000	20,000
Hunton (Devonian)	0	13,800
Hunton (Devonian)	4,600	17,500
Edwards (Cretaceous)	0	11,000
Edwards (Cretaceous)	3,300	13,500
Slate and shale	0	7,500–15,400
Sandstone	0	4,600–14,100
Shale and sandstone		
Devonian	2,000–3,000	13,400
Pennsylvanian	2,000–3,000	11,200
Permian	2,000–3,000	10,000
Cretaceous	2,000–3,000	9,300
Eocene	2,000–3,000	9,000
Pleistocene-Oligocene	2,000–3,000	7,200
		Transverse wave velocity, V_T, ft/sec
Granite	0	6,900–10,800
Norite, Sudbury	0	11,400
Dolomitic limestone	0	10,700
Gabbro, Mellen	L0	11,100
Gabbro, Mellen	L5,000	12,000
Gabbro, Mellen	L40,000	12,200
Diabase, Vinal Haven	L0	10,400
Diabase, Vinal Haven	L5,000	12,600
Diabase, Vinal Haven	L40,000	12,800
Sandstone, quartzitic	L0	11,100
Sandstone, quartzitic	L5,000	12,700
Sandstone, quartzitic	L40,000	13,400
Slate, Everett, Mass.	L0	9,500
Slate, Everett, Mass.	L40,000	10,500

* From Birch's "Handbook of Physical Constants," 1942.

† The depths preceded by L (laboratory) were artificially reproduced in high-pressure apparatus in which the velocities were obtained by dynamical methods.

[a]Reprinted from pg. 22 of Dobrin[1].

Appendix B
Example Problem

This appendix contains a hypothetical set of time-distance curves which are intended to illustrate some of the points in this report. The travel times were synthesized from a known geologic profile, and the interpretation of the time-distance curves can therefore be compared with the original profile.

Assume the following circumstances: We are exploring the foundation conditions for a large dike, and our primary interest is depth to rock, although the thicknesses and velocities of any intermediate layers are also of interest. Similar exploratory work in a nearby area indicates that we can expect sandstone overlain by a glacial till with a sandy overburden. A refraction line with 50-ft geophone spacing has been surveyed, with shots fired at the ends (15-ft offset), at the middle, and at one intermediate point. Shot depths were about 2 ft and can be considered negligible. There is no drilling information anywhere on the line.

The travel times we observed are tabulated in Table B1 and are plotted in Fig. B1.

Table B1. Observed travel times.

Geophone station (ft)	Arrival times (msec)			
	Shot at Sta. 0	Shot at Sta. 125	Shot at Sta. 275	Shot at Sta. 550
0	6	33	50	76
50	16	25	45.5	71
100	28	10	42	67.5
150	37	10	35	60.5
200	42	24.5	24.5	50
250	47	34	10	46.5
300	53.5	—	10	41.5
350	60.5	—	27.5	37
400	61.5	—	29.5	28
450	65.5	—	33.5	20.5
500	71.5	—	38.5	12
550	76	—	44.5	6

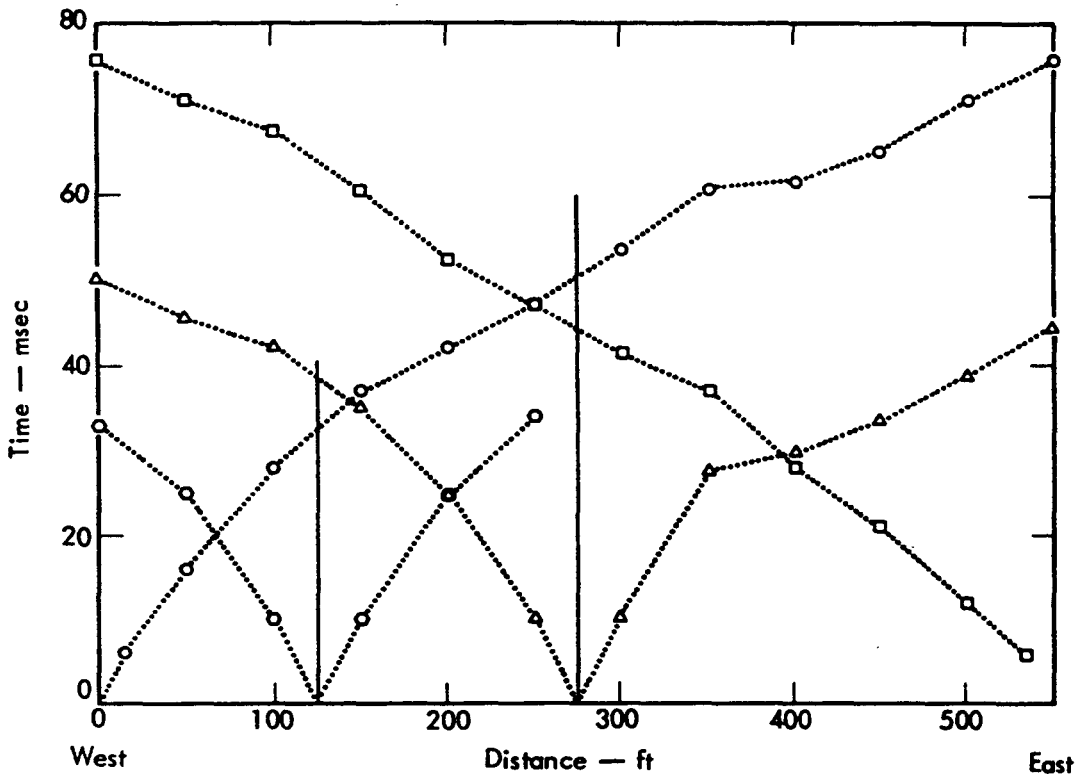

Fig. B1. Travel times observed in hypothetical exploration program.

The first step is to try to identify the various layers according to their velocities. In Fig. B2 straight lines have been drawn through those arrival times that are initially believed to be refractions from the same layer. . The apparent velocities that result from this procedure would indicate that we have a three-layer situation: a; first layer with a velocity of 2,500 to 2,700 ft/sec, an intermediate layer with apparent velocities of 4,100 to 6,400 ft/sec, and a bottom layer (rock) with a velocity that lies somewhere between 8,900 and 10,000 ft/sec.

Although an intermediate layer is clearly indicated on the western half of the line, the situation is not as straightforward towards the east; the end shot at Station 550 shows a 6,000-ft/sec line-up of points, but the middle shot does not indicate the presence of an intermediate layer towards the east. An intermediate shot at Station 425 would have helped resolve this, but, for the sake of our illustration, we are assuming that we did not fire one. For the present, we can pass over this point and go on to refine our velocity values.

The first layer velocities show little variation along the line and a simple average will be adequate; i.e.,

$V_1 \cong 2{,}558$, say 2,550 ft/sec.

On the western half of the line we can compute two values of V_2 by taking harmonic means; i.e.,

$$V_2 \simeq \frac{2 \times 4{,}100 \times 6{,}400}{4{,}100 + 6{,}400} = 4{,}998,$$

say 5,000 ft/sec

$$V_2 \simeq \frac{2 \times 4{,}900 \times 5{,}600}{4{,}900 + 5{,}600} = 5{,}227,$$

say 5,225 ft/sec

and averaging these values with the 6,000 ft/sec on the eastern half, we obtain:

$V_2 \cong 5{,}408$, say 5,400 ft/sec.

The value of V_3 will be determined in the next diagram, but first we proceed to compute delay times or half intercept times for the first layer wherever we can. (Remember that half intercept times and delay times are equivalent if the shot depths are negligible.) Half intercept times are available at Stations 0, 125, 275, and 550. We can compute delay times at Stations 50, 200, and, for the present, at Station 400. All of these times are shown in Fig. B2. For the intermediate stations we will have to interpolate between the values above.

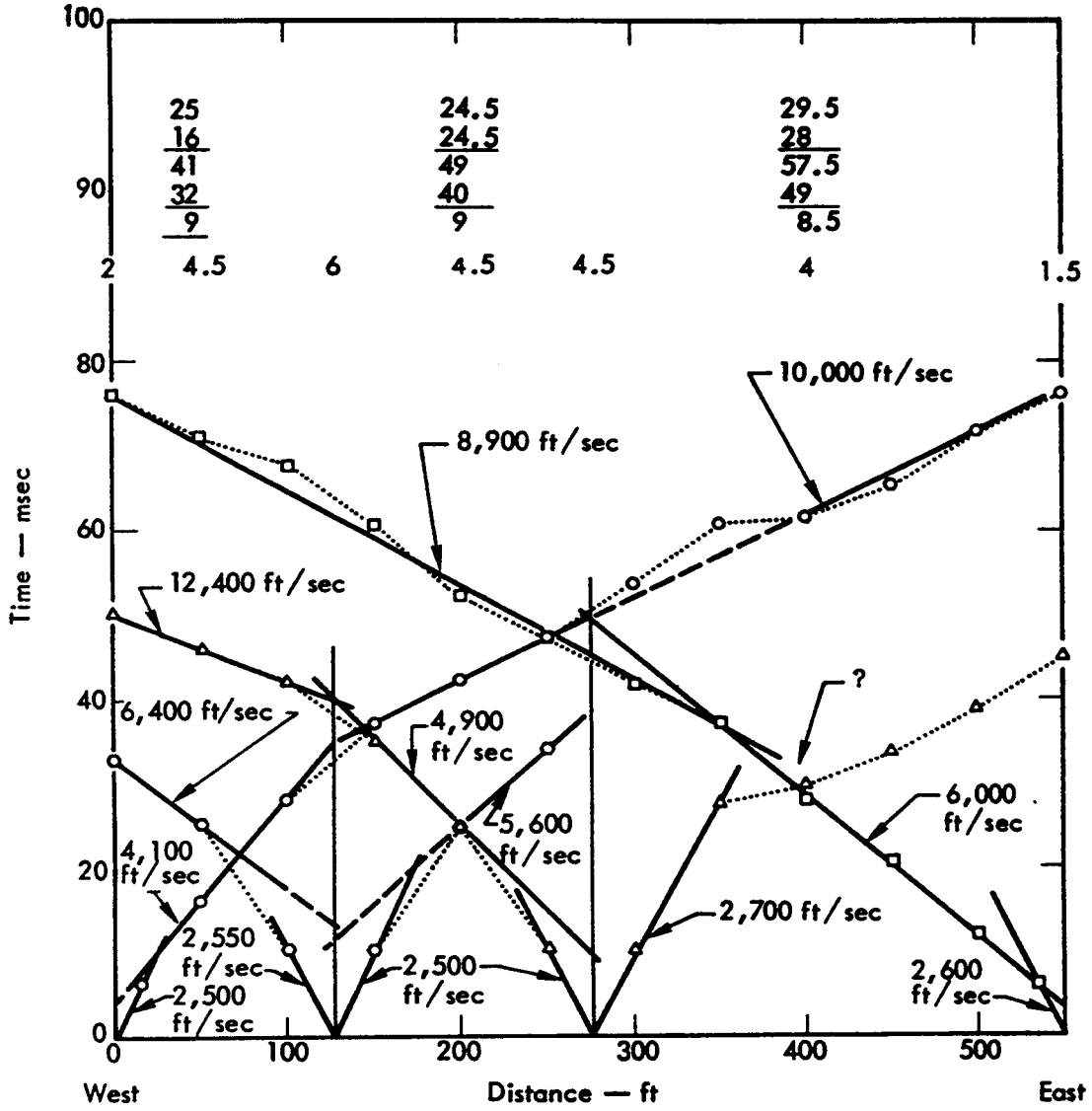

Fig. B2. Identifying layers by velocity and determining half-intercept times and delay times for first layer.

Our next step is to plot the differences in arrival times for the two end shots. This procedure should tell us which times represent refractions from the rock, and what the rock velocity is.

The plot of differences in Fig. B3 results in a value for V_3 of 9,000 ft/sec and suggests that Stations 200 through 450 recorded refractions from the rock from both end shots. Points that do not fall on the line mean that they are differences of arrival times from different layers (assuming no lateral velocity variations in the rock).

Feeling reasonably confident that the arrivals from both directions at Stations 200 through 450 are refractions from the top of the rock, we can proceed to compute delay times at these stations. The computations are shown in Fig. B3. Remember that these times are the combined delay times for the first and second layers (i.e., ΔT_{12}).

As was done in Fig. 12, we reduce the arrival times by the corresponding delay times, obtaining reduced arrival times that now line up at the true refractor velocity. Extending these lines allows us to read off delay times for the remaining geophones. The fact that the line through one set of reduced arrivals has a reciprocal slope of 9,200 ft/sec and the other 9, 000 ft/sec is because of normal scatter, we will use 9, 000 ft/sec for V_3 which was obtained from the difference plots.

We are ready to compute layer thicknesses, but first refer back to Fig. B2 where we computed a first-layer delay time at Station 400. We have just demonstrated that the arrival at Station 400 from the shot at Station 550 is really a refraction from the top of the rock; therefore; this first-layer delay time is not valid and we will have to interpolate between the half intercept times at Stations 275 and 550. Also, the 6,000 ft/sec that we attributed to the second layer at the east end of the line is really an apparent velocity for the rock; however, the arrival at Station 500 from the end shot at Station 550 is a legitimate refraction from the second layer and the 6,000 ft/ sec is still valid.

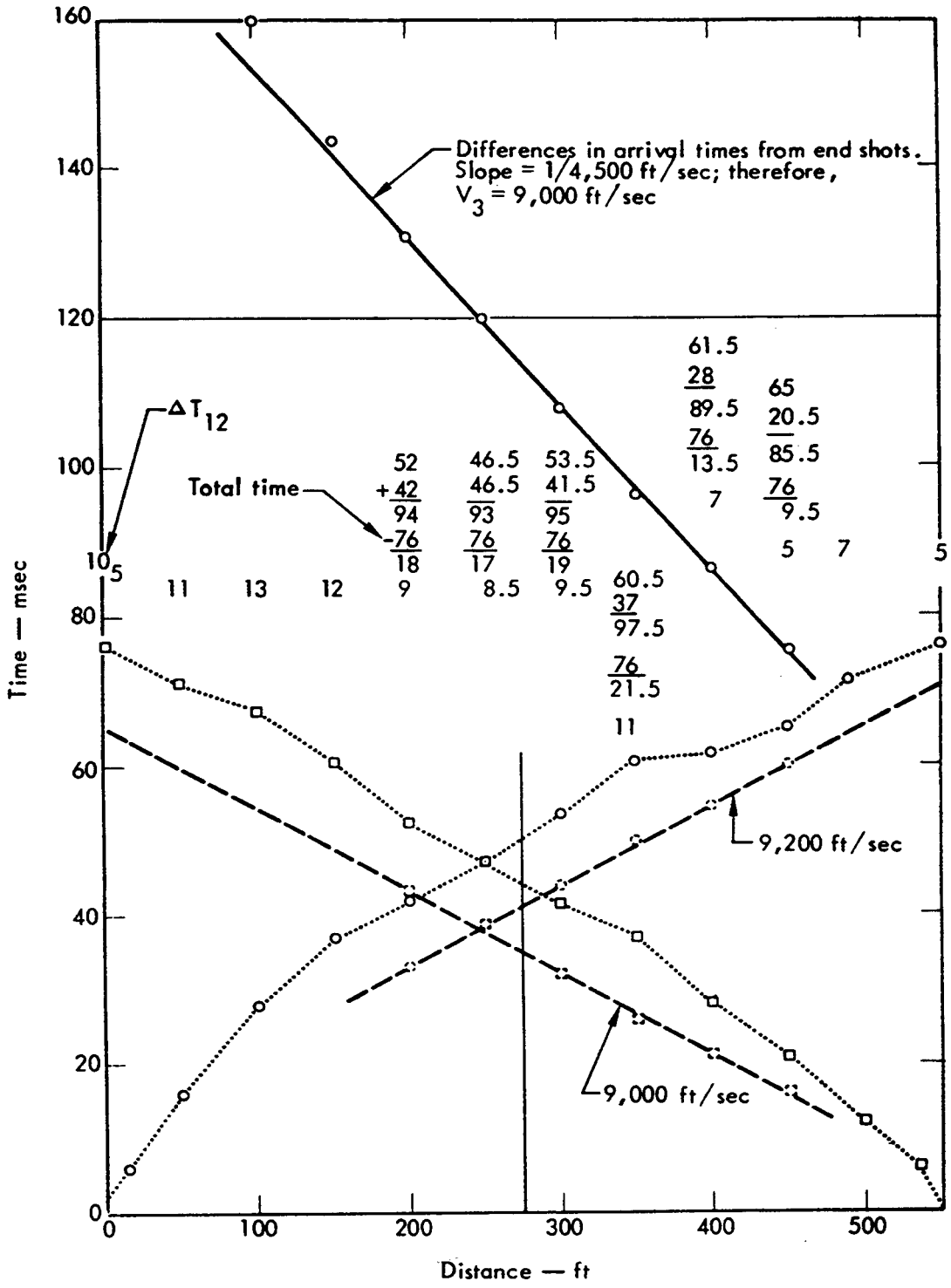

Fig. B3. Determination of true value of V_3 and delay times ΔT_{12} (intermediate shots not shown for sake of clarity).

Let us now assemble all of our information in Table B2.

Figure B4 is a comparison of the foregoing interpretation with the original model from which the travel times .were derived. A number of significant points are apparent. The velocity values of $V_1 = 2{,}500$, $V_2 = 5{,}400$, $V_3 = 9{,}000$ ft/sec determined in the interpretation are in good agreement with the actual values used in the synthesis. Agreement between actual depths and those computed in the interpretation is very good over the western half of the line, but it is not as good on the eastern half. The reason for firing intermediate shots should now be apparent; only because of the shots at Stations 125 and 275 were we able to follow variations in the depth of the over-burden along the western half. The delay times in the overburden are a significant proportion of the total delay time, and any errors in these times are compounded when the difference $\Delta T_{12} - \Delta T_1$ is multiplied by the higher velocity of the underlying layer. Without an intermediate shot between Stations 275 and 500, we had no choice but to interpolate linearly the half intercept times between these points, and consequently there was no way of knowing that the overburden thickened appreciably near Stations 300 and 350.

Table B2. Velocities, cosines, times, and thicknesses.

$$\left.\begin{aligned} V_1 &= 2{,}550 \text{ ft/sec} \\ V_2 &= 5{,}400 \text{ ft/sec} \end{aligned}\right\} \quad \alpha = \sin^{-1} V_1/V_2 \simeq 28 \text{ deg}, \quad \cos\alpha = 0.88$$

$$\left.\begin{aligned} V_3 &= 9{,}000 \text{ ft/sec} \end{aligned}\right\} \quad \beta = \sin^{-1} V_2/V_3 \simeq 37 \text{ deg}, \quad \cos\beta = 0.80$$

Times, T (msec) or thicknesses, Z (ft)	Geophone station (ft)											
	0	50	100	150	200	250	300	350	400	450	500	550
ΔT_1 (or 1/2 T_{12})	2	4.5	6	6	4.5	4.5	4.5	—	—	—	—	1.5
Interpolated ΔT_1's	—	—	—	—	—	—	—	4	3.5	3	2	—
ΔT_{12}	10.5	11	13	12	9	8.5	9.5	11	7	5	7	5
$\Delta T_2 = \Delta T_{12} - \Delta T_1$ [a]	8.5	6.5	7	6	4.5	4	5	7	3.5	2	5	3.5
$Z_1 = \Delta T_1 V_1/\cos\alpha$	6	13	17	17	13	13	13	12	10	9	6	4
$Z_2 = \Delta T_2 V_2/\cos\beta$	57	44	47	41	30	27	34	47	24	14	34	24
$Z_1 + Z_2$	63	57	64	58	43	40	47	59	34	23	40	28

[a] The existence of a positive value for ΔT_2 (i.e., $\Delta T_{12} - \Delta T_1$) for every geophone indicates that the intermediate (5,400-ft/sec) layer is present along the entire profile.

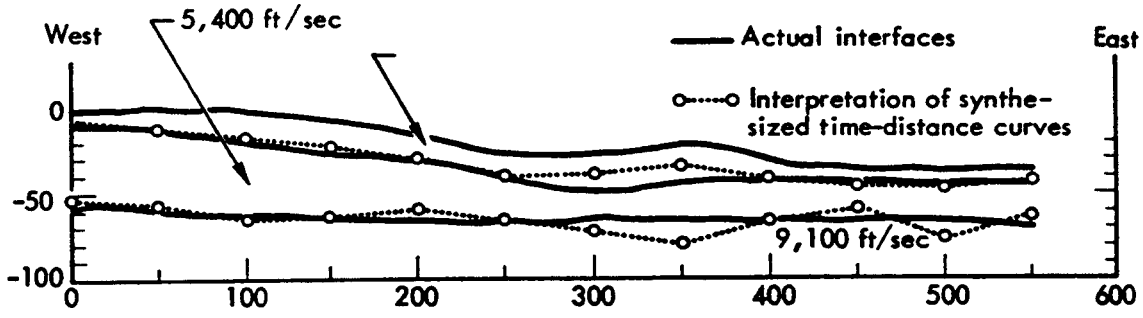

Fig. B4. Original profile compared with and that derived by interpreting synthesized time-distance data.

Printed in the United States of America
Available from
National Technical Information Service
U. S. Department of Commerce
5285 Port Royal Road
Springfield, Virginia 22151